

NAIST-IS-DD1561033

## **Doctoral Dissertation**

# **A computational model for focal brain cooling as a thermal neuromodulation treatment for medically intractable epilepsy**

Jaymar B. Soriano

March 5, 2018

Graduate School of Information Science  
Nara Institute of Science and Technology

A Doctoral Dissertation  
submitted to Graduate School of Information Science,  
Nara Institute of Science and Technology  
in partial fulfillment of the requirements for the degree of  
Doctor of SCIENCE

Jaymar B. Soriano

Thesis Committee:

Professor Kazushi Ikeda	(Supervisor)
Professor Yoshinobu Sato	(Co-supervisor)
Research Associate Professor Takatomi Kubo	(Co-supervisor)
Associate Professor Yuichi Sakumura	(Co-supervisor)
Assistant Professor Adrian Roy Valdez	(University of the Philippines)

# A computational model for focal brain cooling as a thermal neuromodulation treatment for medically intractable epilepsy\*

Jaymar B. Soriano

## Abstract

An estimated 50 million of world's population is afflicted with epilepsy and 20%-40% of diagnosed cases are found refractory to medical treatment. An alternative therapeutic treatment that has been extensively studied in the past decade is focal brain cooling which has shown consistent success in animal studies and also preliminarily in an intraoperative study with a surgical patient. In most *in vitro* studies, cooling suppresses epileptic discharges by reducing their magnitude and frequency and eventually terminates them. However, *in vivo* experiments with rats showed that epileptic discharges were generally persistent during cooling and some even showed slight increases in frequency. In this study, we utilize a computational approach in understanding the mechanisms of focal brain cooling for thermal modulation of epileptic discharges.

In the first part of the study, we formulated temperature dependence in a neural mass model of epileptic discharges. Based from experimental evidences regarding the effect of cooling on synaptic dynamics of neurons, we assumed a mean-field attenuation of post-synaptic potential by using a  $Q_{10}$  factor in the post-synaptic impulse response function of the neural mass model. Simulated activity showed that a low attenuation could already result in reduction of frequency of discharges but with no significant decrease in magnitude, and termination could

---

\*Doctoral Dissertation, Graduate School of Information Science,  
Nara Institute of Science and Technology, NAIST-IS-DD1561033, March 5, 2018.

be achieved with further attenuation. Persistent discharge activity although suppressed in magnitude was otherwise observed from *in vivo* experiments, which led us to conjecture that a concomitant mechanism opposes the reduction in the average firing frequency. We integrated this in the model by adding a reciprocal  $Q_{10}$  factor in the firing response function. Using both mechanisms, the effect of cooling on epileptic discharges observed from *in vivo* experiments were reproduced. We also explored the possibility that cooling has differential effect on PSP generation mechanisms of different neuronal populations as different neurotransmitters are involved.

In the second part of the study, we explored the applicability of focal cooling for secondary generalized epilepsy in which seizure activity spreads to other brain regions. A coupling model was proposed to simulate the propagation of brain activity between two brain regions encompassing the phenomenon of axonal sprouting. Different types of seizure activity can be initiated in a reciprocally coupled non-pathological neural masses depending on the strength of the coupling parameter. We found that the coupling strength required to propagate epileptic discharge activity from one brain region to another brain region is much lower than the coupling strength required to initiate seizure activity, playing a critical role in the spread of seizure activity in a network of brain regions. Using the temperature-dependent model, simulations show that focal cooling stops the spread of low-frequency epileptiform discharge activity; on the other hand, it increases the strength of coupling required to propagate high-frequency discharge activity to other brain regions. The results suggest feasibility of focal cooling as an effective alternative treatment for medically intractable epilepsy even with secondary generalization.

**Keywords:**

neural mass model, seizure, drug-resistant epilepsy, temperature control

# Contents

<b>List of Figures</b>	<b>v</b>
<b>List of Tables</b>	<b>vii</b>
<b>1 Introduction</b>	<b>1</b>
1.1 Epilepsy and treatment . . . . .	1
1.2 Focal brain cooling as alternative therapeutic treatment . . . . .	2
1.3 Research overview . . . . .	3
1.4 Research contribution . . . . .	4
1.5 Thesis organization . . . . .	6
<b>2 Focal brain cooling experiment in rats</b>	<b>7</b>
2.1 Animal model of epilepsy . . . . .	7
2.2 Focal cooling and EEG recording . . . . .	8
2.3 Data preprocessing . . . . .	9
2.4 Summary of experimental data . . . . .	9
<b>3 Computational model of epileptic discharge activity</b>	<b>12</b>
3.1 Neural mass model . . . . .	12
3.2 Parameter estimation . . . . .	15
3.3 Results of model estimation . . . . .	17
3.4 Discussion . . . . .	19
<b>4 Computational model of focal brain cooling</b>	<b>21</b>
4.1 Formulation of temperature dependence . . . . .	21
4.2 Parameter estimation . . . . .	24
4.3 Results . . . . .	25
4.3.1 Estimation of temperature parameters . . . . .	25

4.3.2	Bifurcation with respect to temperature parameters . . . .	26
4.3.3	Differential effect of temperature on PSP generation . . . .	31
4.4	Discussion . . . . .	34
<b>5</b>	<b>Focal brain cooling for secondary generalized epilepsy</b>	<b>41</b>
5.1	Problem overview . . . . .	41
5.2	Review of coupled neural mass models . . . . .	43
5.3	Proposed coupled neural mass model . . . . .	44
5.4	Results . . . . .	45
5.4.1	Coupling gives rise to seizure activity . . . . .	45
5.4.2	Effective coupling from multiple afferents . . . . .	48
5.4.3	High synaptic gain requires low coupling strength to initiate seizure activity . . . . .	49
5.4.4	Propagation of seizure activity . . . . .	51
5.4.5	Effect of focal cooling on the propagation of seizure activity	53
5.5	Discussion . . . . .	54
<b>6</b>	<b>Conclusion</b>	<b>58</b>
6.1	Summary . . . . .	58
6.2	Recommendations . . . . .	60
6.3	Pipeline for proposed thermal neuromodulation . . . . .	61
	<b>References</b>	<b>65</b>
	<b>Publication List</b>	<b>77</b>

# List of Figures

1.1	Implantable brain cooling device in rats . . . . .	3
1.2	Fluorescence imaging of synaptic terminals during cooling . . . . .	5
2.1	Focal brain cooling setup . . . . .	8
2.2	Experimental data . . . . .	10
2.3	Magnitude and frequency of epileptic discharges before and during cooling . . . . .	11
3.1	Neural mass model by Wendling et al. . . . .	14
3.2	Activity map simulated using the neural mass model by Wendling et al. . . . .	15
3.3	Illustration of the Dividing Rectangle algorithm . . . . .	17
3.4	Estimation of Wendling et al. model from activity before cooling .	18
3.5	Symmetry or asymmetry of discharge activity with respect to baseline	20
4.1	Response functions and the effect of $Q_{10}$ . . . . .	22
4.2	Effect of $Q_{10,syn}$ . . . . .	23
4.3	Effect of $Q_{10,syn}$ and $Q_{10,int}$ . . . . .	27
4.4	Comparison of models based on MAPE . . . . .	28
4.5	Bifurcation with respect to $Q_{10,int}$ . . . . .	29
4.6	Bifurcation with respect to $Q_{10,int}$ at different temperature and $Q_{10,syn}$ values . . . . .	30
4.7	Numerical continuation of the noiseless model . . . . .	31
4.8	Simulated activity from rat 4 . . . . .	33
4.9	Simulated activity from rat 1 . . . . .	34
4.10	Contribution of population activity to LFP at different $Q_{10,int}$ . . .	39

5.1	Activity map from reciprocally coupled neural masses with varying values of $g_d$ and $K$ . . . . .	46
5.2	Simulated activity of coupled neural masses with increasing values of $K$ . . . . .	47
5.3	Seizure activity with respect to $K$ . . . . .	48
5.4	Seizure activity initiation from multiple afferents . . . . .	50
5.5	Activity map from reciprocally coupled neural masses with varying values of $G_d$ and $K$ . . . . .	51
5.6	Propagation of pathologic discharge activity . . . . .	52
5.7	Initiation and propagation of discharge activity in a grid network of neural masses . . . . .	53
5.8	Effect of focally cooling the pathologic brain region on the propagation of seizure activity . . . . .	55
6.1	Pipeline for proposed thermal neuromodulation . . . . .	62

# List of Tables

3.1	Description of model parameters and adopted values . . . . .	16
3.2	Estimated values of the parameters for the model of discharge activity before cooling . . . . .	18
4.1	Estimated values of $Q_{10}$ factors from SYN_INT model . . . . .	26
4.2	Estimated values of $Q_{10}$ factors from two other models . . . . .	32

# 1 Introduction

## 1.1 Epilepsy and treatment

The World Health Organization identifies epilepsy as one of the most common neurological diseases affecting approximately 50 million people across all ages across the world [1]. According to the International League Against Epilepsy, a patient has epilepsy if he has had a seizure and his brain activity demonstrates a pathologic and enduring predisposition to have recurrent seizures [2]. Epileptic seizures are a result of abnormalities in brain's electrical activity which can consist of impaired higher mental function or altered consciousness, involuntary or cessation of movement, sensory or psychic experiences, or autonomic disturbances [3]. Because of the risks involved with unanticipated seizures, treatment of the disease is required to improve long-term quality-of-life of the patients.

Antiepileptic drugs such as anticonvulsants are usually given as first line treatment after being diagnosed with epilepsy. Pharmaceutical researches continually seek antiepileptic drugs that are more effective and have less side effects [4, 5]. However, 20%-40% of patients diagnosed with epilepsy are found refractory to antiepileptic drug treatment [6, 7]. Thus, alternative treatments are still being sought after [8, 9]. Surgical treatment, which requires pre-surgical diagnosis, is done by performing a resection of the epileptic foci of the brain. Absolute remission however is not guaranteed, let alone possibilities of unintended outcomes since the method is largely invasive [10, 11]. Although the success rate of surgical treatment is high, limitation in indication and cost significantly hinder medically-intractable epilepsy patients in acquiring it. Another increasingly attractive treatment option involves electric or magnetic stimulation of specific neural region of the brain such as deep brain stimulation and vagus nerve stim-

ulation respectively. These neuromodulation therapies are still under extensive study [12, 13].

## 1.2 Focal brain cooling as alternative therapeutic treatment

In the previous decade, focal cooling of the epileptic brain area has been pursued as an alternative therapeutic treatment for epilepsy and other seizure-inducing brain injuries [14–16]. Studies in animals have shown that reversible cooling to a temperature as low as 15°C using an implantable cooling device (Figure 1.1) is able to terminate epileptic discharges without affecting the normal brain tissue [17–20]. Earlier experiments even noted that focal cooling of the cortex for one hour above 0°C did not induce any irreversible histological change or motor dysfunction [21]. Focal cooling at 25°C was also demonstrated to suppress epileptic discharges in an intraoperative study with a human brain [22]. Epileptic seizures arising from post-traumatic brain injuries were also shown to be suppressed and can be further prevented by moderately cooling the brain down by a temperature reduction of 2°C [23]. In other studies, focal brain cooling has found potential use for treatment of other brain diseases such as ischaemia, stroke, and neonatal encephalopathy [24–27].

The ultimate goal of focal brain cooling studies especially for epilepsy is to develop a technique for epileptic seizure suppression by a temperature control, when detected, via an implantable cooling device as a solution for thermal neuromodulation. This is feasible if we have precise knowledge of how temperature can suppress or terminate seizures. While temperature effects on physiological properties of animal neurons have been well-studied *in vitro* [28–32], mechanisms of how cooling suppresses epileptic discharges especially *in vivo* are still not clearly understood.

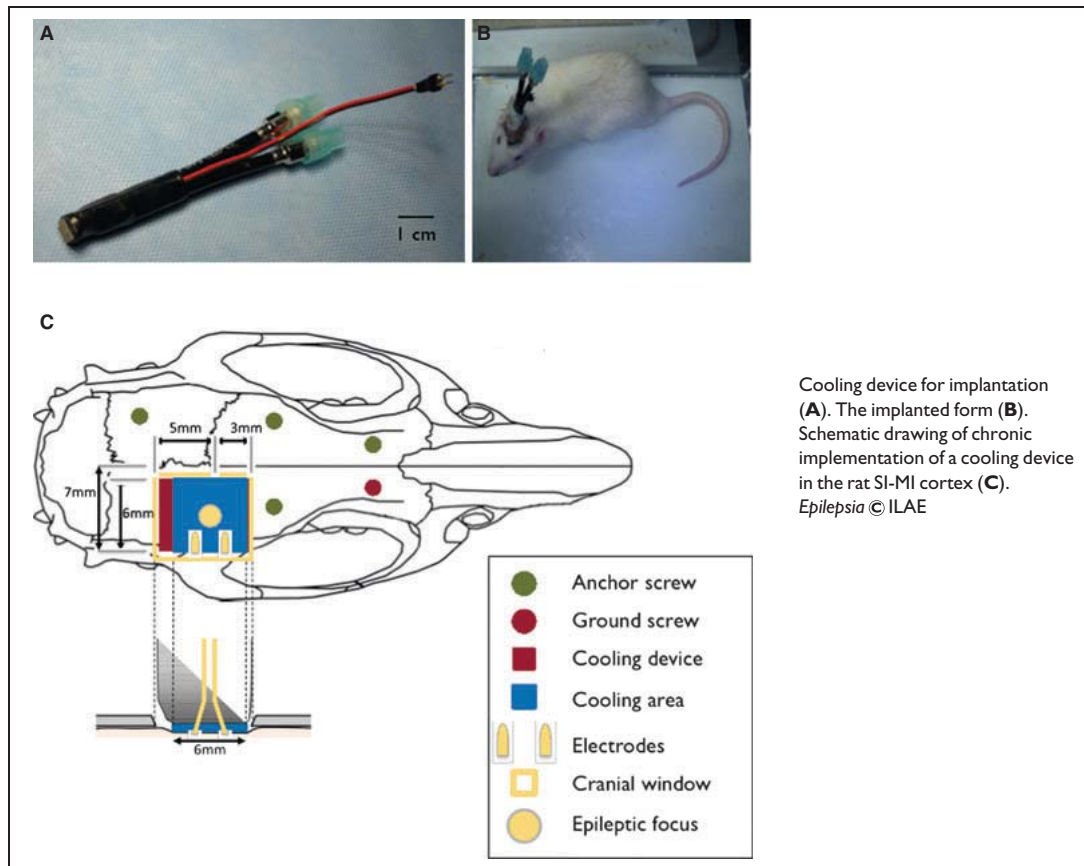


Figure 1.1: Implantable brain cooling device in rats. (Figure from [18].)

### 1.3 Research overview

In this study, we aim to identify prospective mechanisms of cooling and investigate them using a computational modelling approach. Neural mass models have been widely utilized to study brain activities [33–38] and gain bio-physiological insights from them. The model introduced by Wendling et al. in particular was shown to produce different types of brain activities similar to intracranial EEG recordings from epilepsy patients. We explore prospective mechanisms of cooling on epileptic discharges by introducing temperature dependence in the neural mass model of Wendling et al. in light of findings observed from *in vitro* and *in vivo* experiments published in literature. In particular, changes in synaptic dynamics (Figure 1.2) were reported from *in vitro* cooling experiments such as

reduction in the efficacy of neurotransmitter vesicle release [39], loss of dendritic spines [40] and reduced glutamate concentrations [41, 42], suggesting a possible synaptic mechanism. A recent study with patients with intractable epilepsy also reports reduced extracellular glutamate and GABA concentrations during focal brain cooling [43].

We then formulated temperature dependence in our chosen neural mass model by introducing a temperature factor in the post-synaptic impulse response function. Parameter estimation of the model is performed using EEG recordings from *in vivo* cooling experiments with an animal model of epilepsy. Although the model is able to reproduce termination of epileptic discharges reported in *in vitro* studies [44, 45], the results of modelling our *in vivo* experimental data reveal that this synaptic mechanism is not sufficient to explain epileptic discharges that were persistent during cooling although suppressed in magnitude (see Chapter 2). We propose that another mechanism is required to compensate the effect of this synaptic mechanism to be able to reproduce observed suppression of epileptic discharges during cooling in terms of reduction in both frequency and magnitude of discharges. We discuss some biological plausibility of this compensatory mechanism based from published results from cooling experiments. The temperature dependence is in the form of a temperature coefficient ( $Q_{10}$ ) which represents the factor by which the rate of a process increases for every ten-degree rise in the temperature at which it takes place [46]. In this study, the  $Q_{10}$  values determine whether suppression or termination of epileptic discharges can be achieved. Such heterogeneous response of epileptic discharge activity to cooling is revealed by bifurcation patterns found using numerical continuation.

## 1.4 Research contribution

Alternative treatment for medically intractable epilepsy will be available in the future that will significantly reduce cost and risk involved compared to surgery. In collaboration with neurosurgeons from Yamaguchi University School of Medicine under the Japanese Consortium for Advanced Epilepsy Treatment (CADET) Project, our study attempts to start an initiative on thermal neuromodulation

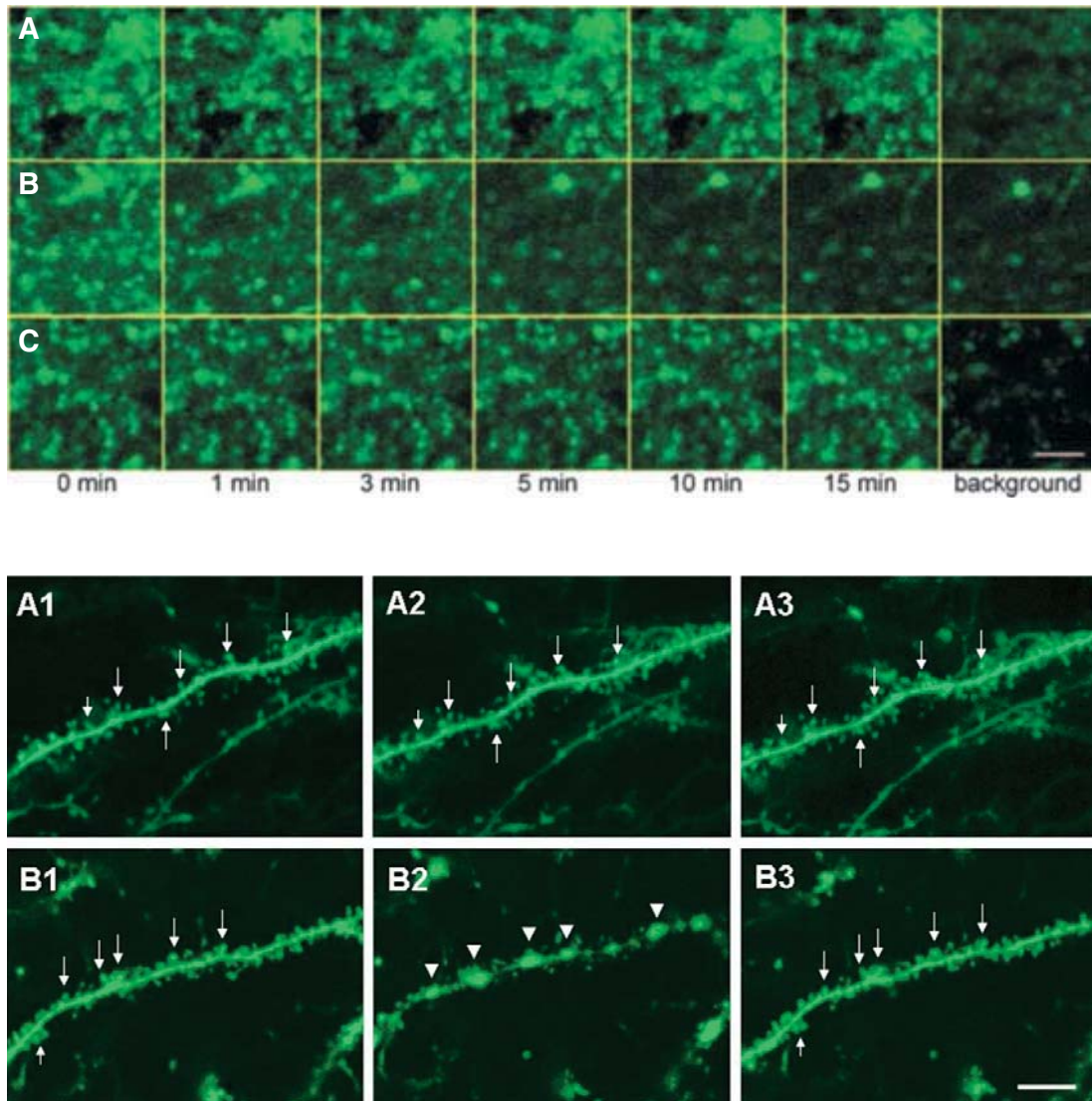


Figure 1.2: Fluorescence imaging of synaptic terminals during cooling. (Top) Reduction in neurotransmitter concentrations in presynaptic terminal (Figure from [39]). (Bottom) Loss of dendritic spines in post-synaptic terminal (Figure from [40]).

of epileptic brain activity using a computational approach that can soon be validated with animal experiments and clinical tests.

## 1.5 Thesis organization

This thesis is organized as follows:

- Chapter 2 describes the experimental data used in the study.
- Chapter 3 discusses the neural mass model used to simulate the epileptic discharge activity of the animal model of epilepsy.
- Chapter 4 presents our formulation of temperature dependence in the neural mass model together with an analysis of the model estimation results and a discussion of the physiological plausibility of the formulated model.
- Chapter 5 takes up on the second part of the study which extends on the case of a spreading seizure activity and how thermal neuromodulation can be possible.
- Chapter 6 ends the thesis with a conclusion and recommendations about what can be pursued as future direction of the study.

## 2 Focal brain cooling experiment in rats

Focal brain cooling experiments were performed at Yamaguchi University School of Medicine. The study utilized their data for parameter estimation of our model. All experiments were performed according to the Guidelines for Animal Experimentation of Yamaguchi University School of Medicine. The following sections describe the animal model of epilepsy used and experimental setup of focal brain cooling taken from [47], preprocessing procedure, and a summary of the preprocessed experimental data.

### 2.1 Animal model of epilepsy

Male Sprague-Dawley rats, 11-12 weeks old at the start of the study, were anaesthetized with urethane (1.25 g/kg, i.p.). Lidocaine, a local anaesthetic, was applied at pressure points and around the area of surgery. After initial surgery, the animals were fixed in a stereotaxic apparatus (SR-6, Narishige Co., Tokyo, Japan). Body temperature was maintained at  $37\pm 1^\circ\text{C}$  with a heating pad (BWT-100, Bio Research Center Co., Japan). The depth of anaesthesia was monitored throughout the experiment by testing for reflexes and monitoring changes in heart rate in response to tail pinching.

Penicillin G potassium (Sigma, Japan) was dissolved in 0.9% saline at a concentration of 400 IU/l. A rectangular opening (4mmx10 mm) in the cranium was made above the left sensorimotor cortex to allow insertion of a guide cannula. Penicillin G potassium was administered into the left sensorimotor cortex for 5 min at a rate of  $5\mu\text{l}/\text{min}$  (total 2000 IU). Administration was performed via a  $10\mu\text{l}$

Hamilton syringe (MS-10 type, Ito Corp. Fuji, Japan) attached to a microinfusion pump (ESP-64, Eicom, Japan), after the dura-arachnoid membrane had been carefully incised at the point of entry of the needle. The stereotactic coordinates relative to the bregma were 1 mm (posterior) and 3 mm (lateral).

## 2.2 Focal cooling and EEG recording

The cooling device was placed on the dura-arachnoid membrane. A thin thermocouple (IT-24, Physitemp, Japan) was placed between the cooling device and the brain surface. A small slit in the dura was made and the injection cannula (0.4mmx19mm, NN-2719S, Terumo, Japan) was inserted at a depth within 1 mm from the brain surface. An Ag/AgCl electrode for recording EEG (Unique Medical Co., Fukuoka, Japan) was positioned stereotactically 2 mm below the cortical surface at the left sensorimotor cortex just beneath the cooling device. A reference electrode was inserted in the neck muscle and EEG were recorded continuously by a digital electroencephalograph (GE Healthcare, Japan). The conditions for recording EEG were namely: time constant: 0.3 s; high-frequency filter: 10 kHz; notch filter: on. Five different rat experiments each were done at cooling temperatures 25°C, 20°C, and 15°C.

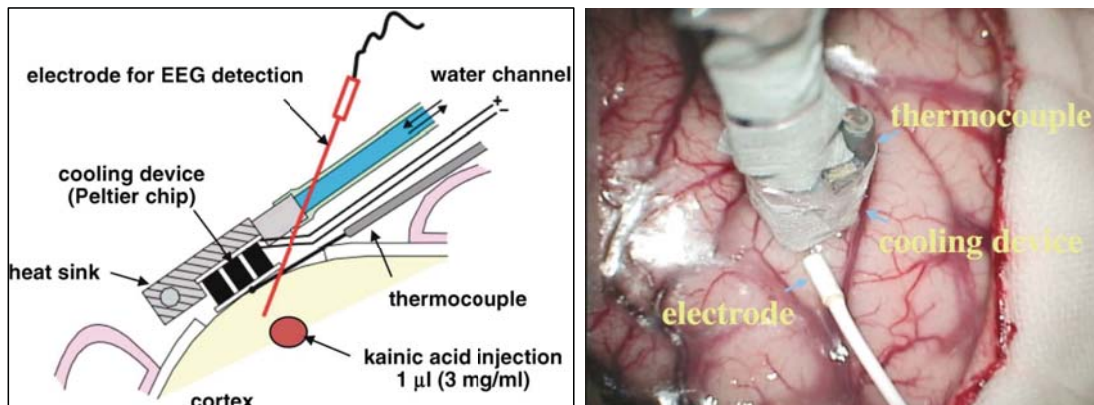


Figure 2.1: Focal brain cooling setup. Schematic setup of focal brain cooling (left) and an actual setup in a human brain intraoperative study (right). (Figures are taken from [22].)

## 2.3 Data preprocessing

To remove high frequency components, the raw recordings underwent a 40-Hz low-pass filter using a fifth order Butterworth filter in Matlab<sup>®</sup>. The frequency range [0-40] Hz also matches the represented frequencies in the model. One-minute steady-state intervals before and during cooling were identified by an expert neurosurgeon and were taken from the filtered data for the study. For the model estimation procedure, first, the data is further downsampled to 2kHz corresponding to a step size of 0.5 ms in the model simulation. Next, both the downsampled data and the simulated EEG were normalized by dividing by their respective standard deviations of activity before cooling, thus, they are reported in arbitrary units (au) unless otherwise stated.

## 2.4 Summary of experimental data

Figure 2.2 shows a summary of the preprocessed data in which we concatenated one-minute steady state activities before and during cooling. Suppression of epileptic discharges during cooling was observed especially with 15°C-cooling temperature (Figure 2.2). Epileptic discharges were suppressed in terms of magnitude (lower magnitude during cooling) in all cases. In most cases, frequency of epileptic discharges is lower during cooling, and is slightly higher in some cases. The average magnitude and frequency of epileptic discharges before and during cooling are summarized in Figure 2.3 with error bars indicating minimum and maximum values from five rats. In general, we can say that epileptic discharges were suppressed during focal cooling at all three cooling temperatures. Surprisingly, significant termination of epileptic discharges was observed only in two out of five rats with 15°C cooling temperature compared to most *in vitro* recordings reported in literature; epileptic discharges were generally persistent during cooling from these *in vivo* recordings.

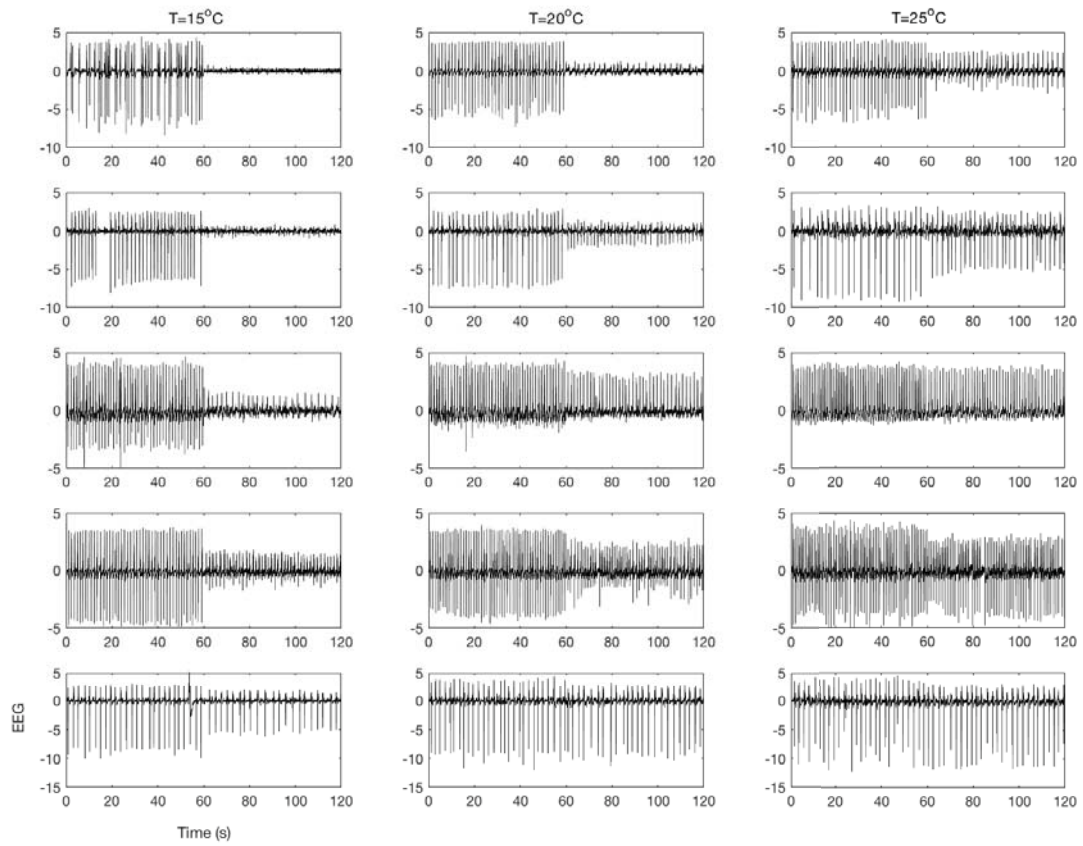


Figure 2.2: Experimental data. Concatenated one-minute steady state activities before (0s-60s) and during (60s-120s) cooling identified by an expert. (From top to bottom: rat 1 to rat 5.)

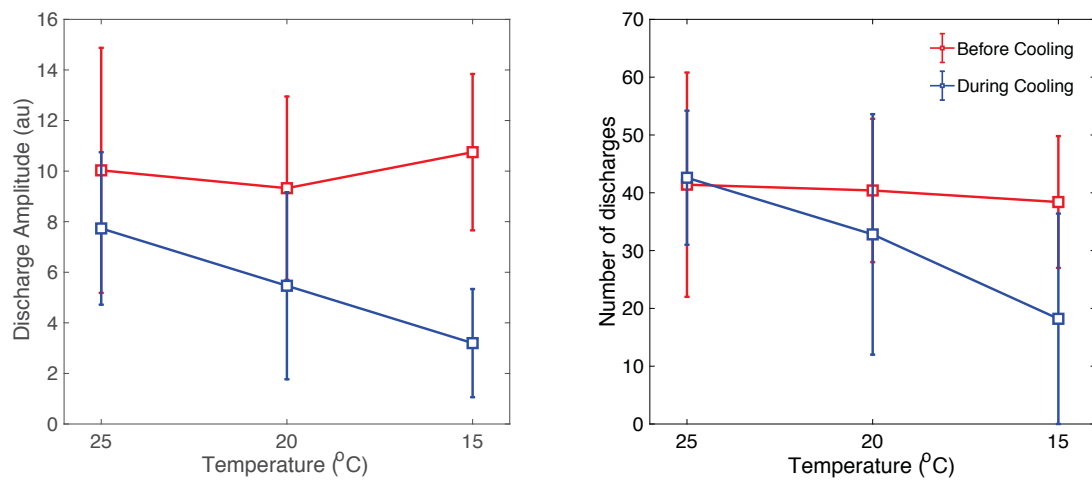


Figure 2.3: Magnitude and frequency of epileptic discharges before and during cooling. Magnitude of epileptic discharges before cooling (red) decreased during focal cooling (blue) in all cases (left). Frequency of epileptic discharges also decreased during cooling in most cases (right) with slight increases seen in some cases (Figure 2.2). Error bars indicate minimum and maximum observations from five rats.

# 3 Computational model of epileptic discharge activity

The following section gives a comprehensive discussion about neural mass models. A particular neural mass model was used to simulate the epileptic discharge activity of the animal epilepsy model used in the study. The parameters of the model were estimated using the experimental data from Chapter 2. Details of the parameter estimation procedure, results, and discussion are given in the succeeding sections.

## 3.1 Neural mass model

Different intracranial EEG activities such as spike-wave discharges and low-voltage high-frequency activity, have been widely explained using neural mass models - a class of models based on a mean-field approximation of the activity of a population of neurons. Neural mass models involve two major processes described by two functions: a firing response function and a post-synaptic impulse response function. The firing response function approximates the average firing rate of a population in response to an average input potential (the average membrane potential of the population). Assuming a unimodal distribution of threshold potentials, the firing response function of a population of neurons can be described by a sigmoid function [48] given by

$$S(v) = \frac{2e_0}{1 + e^{\left(\frac{v_{th}-v}{\sigma_{th}}\right)}}, \quad (3.1)$$

where  $v_{th}$  is the average threshold potential at which the population fires at half the maximum firing rate  $e_0$ . The steepness of the sigmoid curve  $1/\sigma_{th}$  is inversely

related to the variability in thresholds of excitation of neurons in the population [48]. On the other hand, the average post-synaptic potential (PSP) input of a neuronal population to other populations to which it provides excitation or inhibition is given by the convolution of the post-synaptic impulse response function  $h(t)$  of the population and its average firing rate  $u(t)$ . Originally, the post-synaptic impulse response function is modelled using a sum of two exponentials [33] as compared from experimental data but was later simplified to

$$h_X(t) = G_X g_X t e^{-g_X t}; t \geq 0, \quad (3.2)$$

where  $G_X$  is the average post-synaptic gain and  $g_X$  is the reciprocal of the average synaptic time constant of population  $X$ . The convolution  $v_X(t) = h_X(t) * u(t)$  is equivalent to the solution of the following second-order differential equation using Green's Formula [49]:

$$v_X'' + 2g_X v_X' + g_X^2 v_X = G_X g_X u. \quad (3.3)$$

The primary cell population also receives additional noisy input from subcortical afferents and other brain regions which makes the differential equation stochastic. Such can be solved numerically using stochastic methods such as Euler-Maruyama scheme. This noisy input is in terms of firing rate and contributes as excitatory PSP input. Finally, the average membrane potential of a population, which is the input to Eq. (3.1), is taken as the weighted summation of the average post-synaptic potentials of the afferent populations (inhibitory populations have negative contribution). The respective weights are determined by the number of synaptic connections from the afferent populations. The average membrane potential of the primary cell population is taken as representative of the local field potential (LFP) from cortical activity [33].

Different neural mass models vary in terms of the types of neurons that comprise a population and the interconnections among the populations (feedback loops). Da Silva et al. [33] tried to explain alpha rhythm of brain activity by considering two populations: excitatory thalamocortical neurons as primary cell population and a population of inhibitory interneurons. Jansen and Rit [34] extended this model using pyramidal cells as the primary excitatory neurons and

two types of interneurons - excitatory and inhibitory. They also estimated the relations among the number of synaptic interconnections between neuronal populations using animal records of cortical synapses found in literature. Wendling et al. [35] further differentiated slow and fast inhibitory interneurons based on the studies of [50, 51] from hippocampal connections. In their model, slow inhibitory interneurons project to the dendrites while fast inhibitory interneurons project to the soma or near the soma of pyramidal cells. Moreover, slow inhibitory interneurons provide inhibition to fast inhibitory interneurons. Although the model was patterned after neuronal connections in hippocampus, similar architecture has been seen in the neocortex (see [52] for an extensive review). The block diagram of the model is shown in Figure 3.1. The parameters of the model are summarized in Table 3.1 together with the standard values adopted in this study.

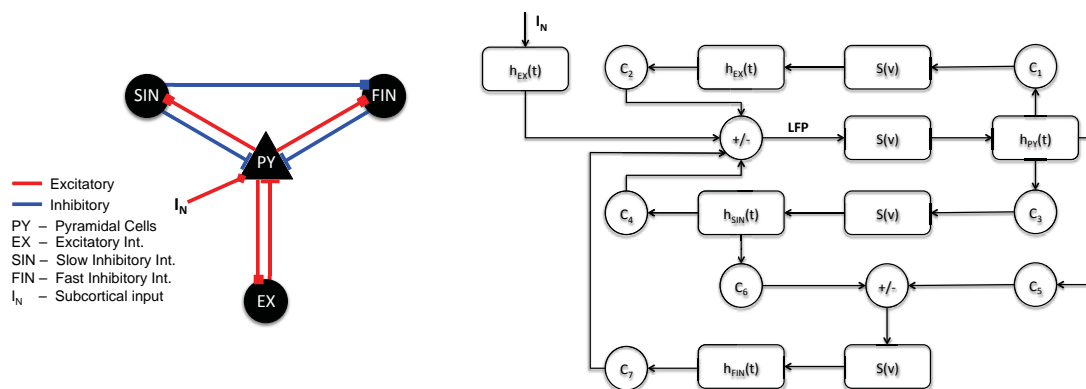


Figure 3.1: Neural mass model by Wendling et al. Block diagram of the model showing the interconnections among the neural populations (left) and the corresponding neural circuit (right).

Wendling et al. showed that their model is able to capture different brain activities observed in intracranial EEG recordings from epilepsy patients [35]. By fixing the value of average excitatory synaptic gain, an activity map (Figure 3.2) shows regions of different brain activities by varying the average synaptic gains of slow and fast inhibitory neuronal populations. They used their model to explain that fast epileptic activity can arise due to impaired GABAergic inhibition by slow inhibitory interneurons. They demonstrated this by estimating average

synaptic gains in the model from intracranial EEG recordings of temporal lobe epilepsy (TLE) patients. In this study, we used the same model and show that it strongly captures the discharge activity of the animal model of epilepsy used in the experiments.

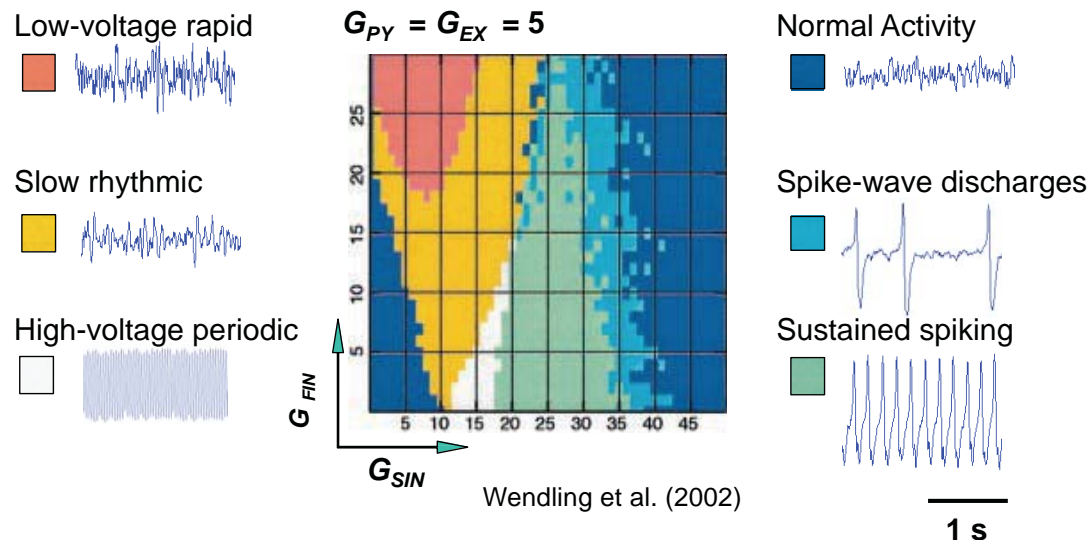


Figure 3.2: Activity map simulated using the neural mass model by Wendling et al. Different brain activities can be simulated by Wendling et al. model by varying average slow and fast inhibitory gains (Center figure from [35]).

## 3.2 Parameter estimation

Since the cooling experiments were performed on five rats, model parameters were estimated per rat from three experiments at different cooling temperatures. Modified from [53], the objective function involved in the estimation is given by

$$J(\theta) = \sum E_{IDI} + E_{EffMag}, \quad (3.4)$$

where  $E_x$  is the mean absolute percentage error (MAPE) of feature  $x$  computed as  $|x_{model} - x_{data}| / |x_{data}|$ . The summation is over the three cooling experiments

Table 3.1: Description of model parameters and adopted values

Parameter	Description	Values adopted in this study
$G$	Average synaptic gain (mV)	$G_{PY} = G_{EX} = 5.0; G_{SIN} \in [25.0, 31.0]; G_{FIN} \in [85.0, 105.0]$
$g$	Reciprocal of average synaptic time constant (Hz)	$g_{PY} = g_{EX} = 100; g_{SIN} = 50; g_{FIN} = 500$
C	Average number of synaptic connections	$C_{PY \rightarrow EX} = 135;$ $C_{EX \rightarrow PY} = 0.8C_{PY \rightarrow EX};$ $C_{PY \rightarrow SIN} = 0.25C_{PY \rightarrow EX}$ $C_{PY \rightarrow FIN} = 0.3C_{PY \rightarrow EX};$ $C_{SIN \rightarrow PY} = 0.25C_{PY \rightarrow EX}$ $C_{FIN \rightarrow PY} = 0.8C_{PY \rightarrow EX};$ $C_{SIN \rightarrow FIN} = 0.1C_{PY \rightarrow EX}$
$v_{th}$	Average threshold potential of firing (mV)	6.0
$2e_0$	Maximum firing rate (Hz)	5.0
$1/\sigma_{th}$	Steepness of sigmoid curve	0.56
$I_N$	Subcortical input firing rate	$\mathcal{N}(\mu = 90, \sigma = 30)$

per rat. The features used in the estimation are the average inter-discharge interval (IDI) over the one-minute series and the effective magnitude (*EffMag*) of epileptic discharges. *IDI* is computed as

$$IDI = \frac{1}{N_D} \sum_{i=1}^{N_D-1} t_{i+1} - t_i, \quad (3.5)$$

where  $t_i$  is a time at which a discharge (exceeding three standard deviations of the activity) occurs, and  $N_D$  is the number of discharges within the one-minute activity. *EffMag*, on the other hand, is defined as

$$EffMag = P_{99} - P_1, \quad (3.6)$$

where  $P_n$  denotes  $n^{\text{th}}$  percentile of the activity. Since the model is stochastic, ten different simulations were taken for each set of parameters from which the MAPE is computed against the experimental data.

Finally, after we are able to narrow down the parameter space to optimize the objective function, a global search is employed [54]. We used Dividing Rectangle (DiRect) method [55, 56], a deterministic global optimization method (illustrated in Figure 3.3) that is less computationally expensive than stochastic evolutionary methods such as Genetic Algorithm which was used in [53]. Moreover, estimation was performed using a one-minute steady-state activity in contrast to short-period dynamic estimation procedures such as Kalman Filtering [57] and Dynamic Causal Model [58].

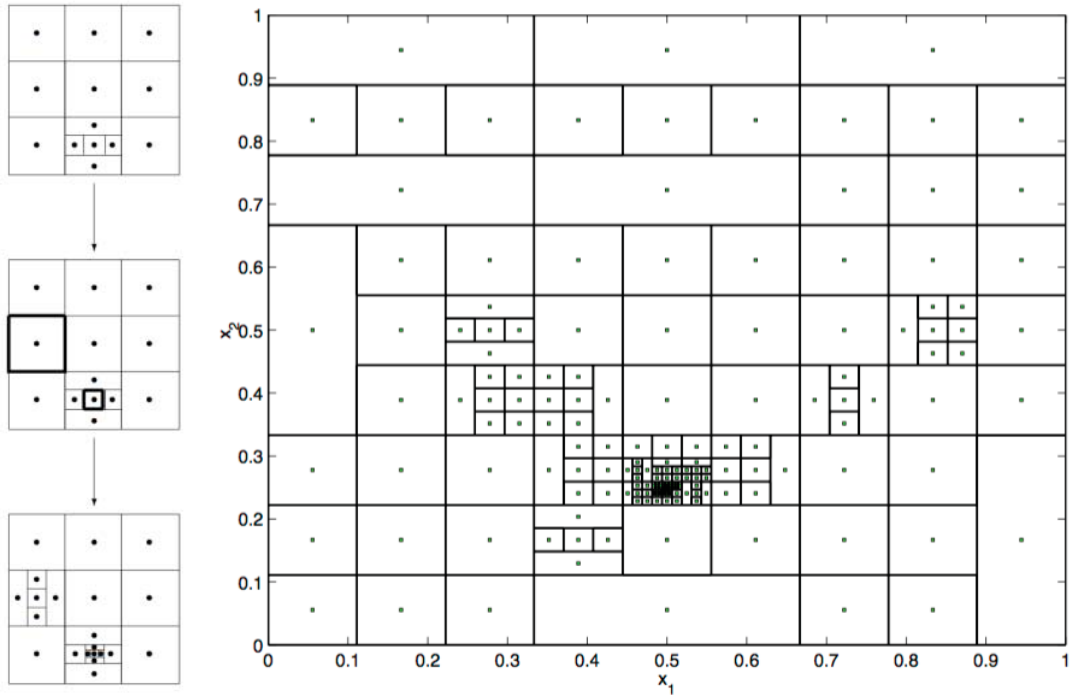


Figure 3.3: Illustration of the Dividing Rectangle algorithm. Dividing rectangle is a deterministic global search algorithm for optimization of a multivariate objective function (Figure from [56]).

### 3.3 Results of model estimation

It is generally accepted that epileptic activity results from changes in excitation-inhibition ratio. In the neural mass model, keeping the average excitation gain constant, excitation-to-inhibition ratio increases as  $G_{SIN}$  or  $G_{FIN}$  is decreased thereby simulating epileptic discharge activity. Exploration of the model shows that EEG recordings from the animal model of epilepsy used in the study are best explained by high average fast inhibitory gain  $G_{FIN}$  and low average slow inhibitory gain  $G_{SIN}$  (Table 3.2). This is consistent with previous findings that epileptic activity can arise when dendritic inhibition is impaired [35]. Figure 3.4 shows a reproduction of epileptic discharge activities before cooling for two of the five rats. We observe that lower values of  $G_{SIN}$  reproduce a discharge activity that is asymmetric with respect to baseline while higher values of  $G_{SIN}$  reproduce a discharge activity that tends to be symmetric with respect to baseline. On the

other hand, increasing both  $G_{SIN}$  and  $G_{FIN}$  reduces the frequency of epileptic discharges by effectively reducing the average membrane potential of the primary cell population which is basically the simulated EEG.

Table 3.2: Estimated values of the parameters for the model of discharge activity before cooling

Rat	$G_{SIN}$ (mV)	$G_{FIN}$ (mV)	MAPE (Min, Max)
1	29.23	86.22	(1.24, 3.93)
2	26.67	97.91	(1.54, 16.33)
3	25.01	101.44	(11.08, 16.54)
4	28.66	87.73	(1.49, 11.72)
5	25.32	102.75	(1.87, 5.44)

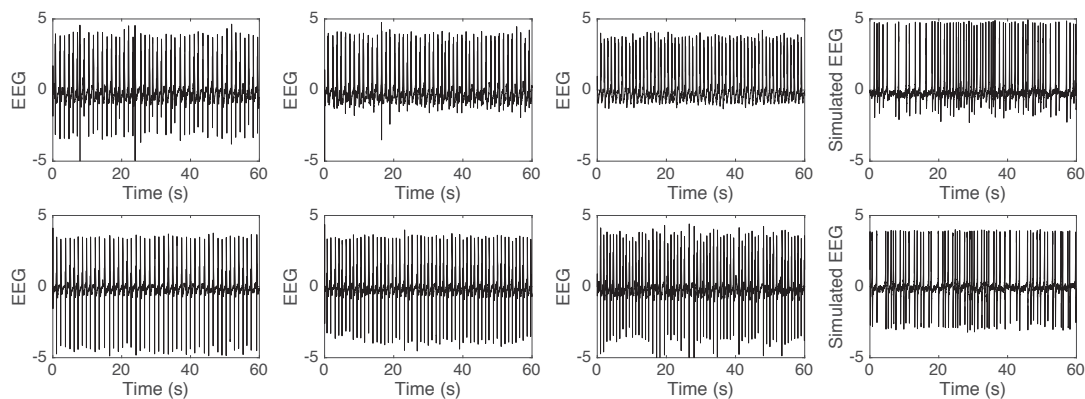


Figure 3.4: Estimation of Wendling et al. model from activity before cooling. Wendling model captures several features of epileptic discharges before cooling such as average inter-discharge interval, discharge magnitude, and asymmetry of epileptic discharges with respect to baseline. Epileptic discharge activity before cooling (left) and simulated activity (right). Top plots are for rat 3 while bottom plots are for rat 4.

### 3.4 Discussion

Estimation results confirm the ability of Wendling et al. model to capture different brain activities particularly epileptic discharge activity induced in the animal model of epilepsy used. After a brute-force search in the  $G_{SIN}$  and  $G_{FIN}$  space (with  $G_{PY} = G_{EX} = 5.0$ ), we find that the epileptic discharge activities from our animal model of epilepsy are best estimated in the range [24.0, 31.0] mV for  $G_{SIN}$  and [80.0, 110.0] mV for  $G_{FIN}$ , the latter of which is not explored in the original study. Alternatively, we can keep  $G_{FIN}$  in standard range [20.0, 50.0] mV but would entail that the number of synaptic connections from fast interneurons to pyramidal cells is twice than the standard value or that the maximum average firing rate of fast inhibitory interneurons is twice than that of the others (see Eq. (3.3)). This is still consistent with the findings of Wendling et al. [35] suggesting that impaired dendritic inhibition alters excitation-inhibition balance giving rise to rhythmic discharge activity capturing the effect of Penicillin G potassium in cortical tissues inhibiting GABA receptors [59]. Nevertheless, the estimated parameters indicate that our animal model of epilepsy can be best explained by much lower dendritic inhibition and much higher perisomatic inhibition compared to the standard range of values reported. High  $G_{SIN}$  values in fact supports [60] which reported high somatic inhibition together with impaired dendritic inhibition in experimental epilepsy.

Meanwhile, asymmetric epileptic discharge activities with respect to baseline activity as seen from experiments with rat 3 can be reproduced with lower value of  $G_{SIN}$  (25.012 mV) and higher value of  $G_{FIN}$  (101.44 mV). On the other hand, symmetric discharge activity with respect to baseline is observed when dendritic inhibition is increased with lower perisomatic inhibition. Figure 3.5 illustrates that this symmetry (asymmetry) of the discharge activity (which is the summation of the average PSP from excitatory and inhibitory interneurons) is largely due to the PSP response of excitatory interneurons showing faster (slower) repolarization while the PSP responses of the inhibitory interneurons do not show significant changes.

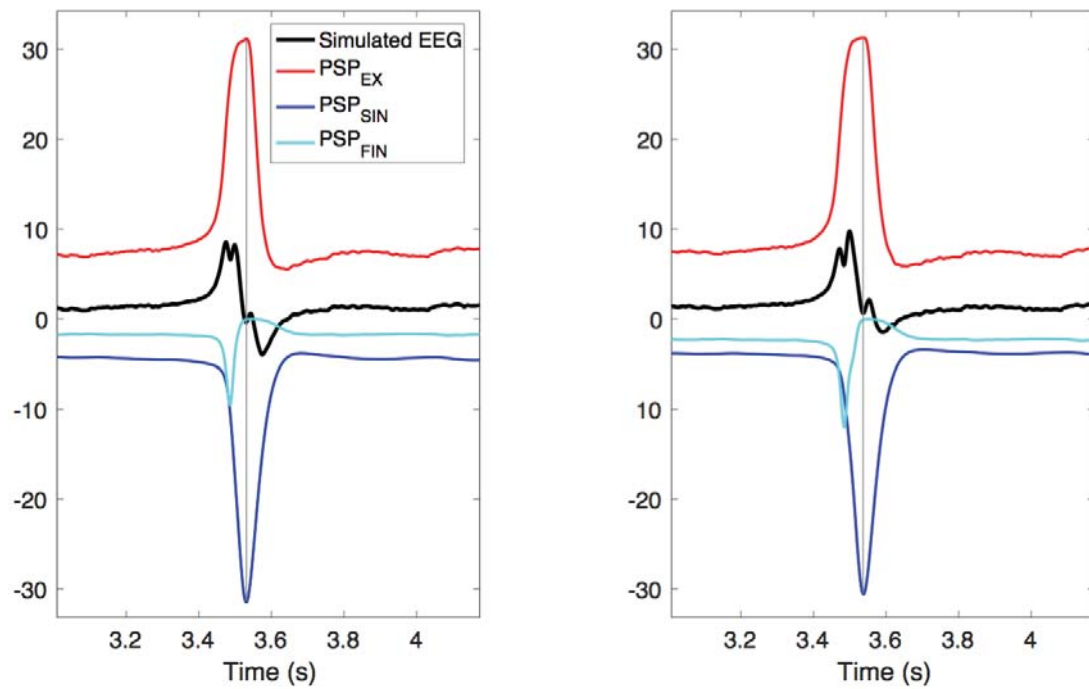


Figure 3.5: Symmetry or asymmetry of discharge activity with respect to baseline. Average PSP from excitatory interneurons determine whether the simulated discharge activity tends to be symmetric (left) or asymmetric (right) with respect to baseline. Gray line indicates that symmetric (asymmetric) discharge activity arises when average excitatory PSP has faster (slower) repolarization.

# 4 Computational model of focal brain cooling

The main component of this study is to construct a computational model for focal brain cooling based from the results of experiments published in literature. In the following section, we discuss our formulation of temperature dependence in the neural mass model presented in Chapter 3. A similar parameter estimation procedure is employed to estimate the temperature parameters introduced in the model. The results of the parameter estimation is presented in the succeeding section followed by a discussion of the bio-physiological implications of the proposed temperature dependent model.

## 4.1 Formulation of temperature dependence

In this study, we try to explain how cooling works in suppressing epileptic discharges by introducing temperature dependence in the neural mass model of Wendling et al. particularly for epileptic discharges. Our formulation starts with reduction in concentration of neurotransmitters as reported in *in vitro* studies. We model this effect as an attenuation factor in the post-synaptic impulse response function. Specifically, we assume a temperature dependence in terms of a  $Q_{10}$  factor as follows:

$$h_X(t) = Q_{10, syn}^{(T-T_0)/10} G_X g_X t e^{-g_X t}; t \geq 0. \quad (4.1)$$

Here,  $T_0$  is the baseline temperature which is 31°C in the experiments. This temperature dependence attenuates the average synaptic gain and thus reduces the average PSP (Figure 4.1) which contributes to the average membrane potential of the population to which it provides excitation or inhibition. For excitatory

and slow inhibitory interneurons, their average membrane potentials are solely contributed by the average PSP from pyramidal cell population, thus, are also attenuated and consequently result in reduced firing frequency. For the pyramidal cell population and fast inhibitory interneurons, negative average inhibitory PSP contributes to their average membrane potential. If the weighted effect (in terms of synaptic connections) of temperature on inhibitory PSP is less than that on excitatory PSP, a net decrease in average membrane potential results. With the parameter values chosen in the model (Table 3.1), this is more likely the case.

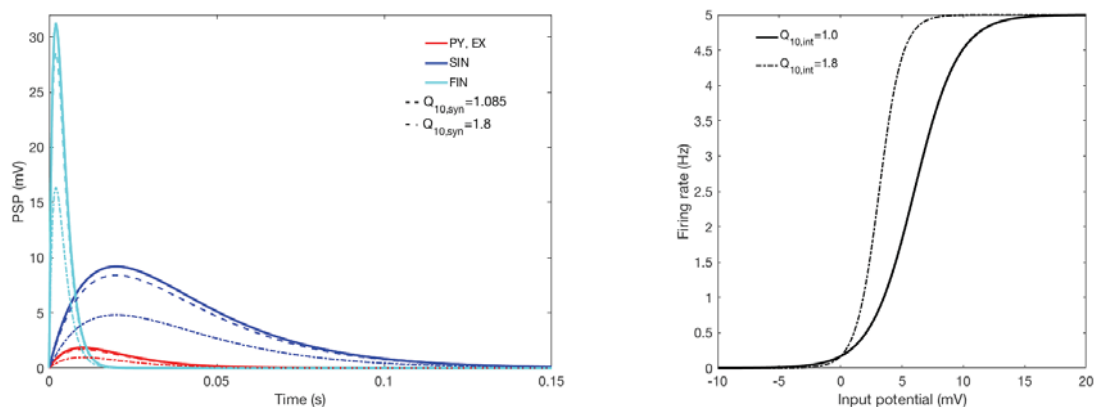


Figure 4.1: Response functions and the effect of  $Q_{10}$ . Different populations of neurons have different post-synaptic impulse response (solid lines, left) but are assumed to have the same firing response (solid line, right).  $Q_{10,syn}$  scales down the post-synaptic impulse response curves (broken lines, left) while  $Q_{10,int}$  changes the properties of the firing response curve (broken line, right).

In Figure 4.2, we can see that as  $Q_{10,syn}$  is increased from unity, frequency of discharges during cooling is decreased until termination. However, the value of  $Q_{10,syn}$  at which termination is nearly achieved ( $Q_{10,syn}=1.085$ ) does not significantly attenuate PSP magnitude (Figure 4.1), consequently the magnitude of isolated discharges. In contrast, persistent discharges were observed during cooling in the experiments (Figure 2.2). These are suggestive that another mechanism is involved.

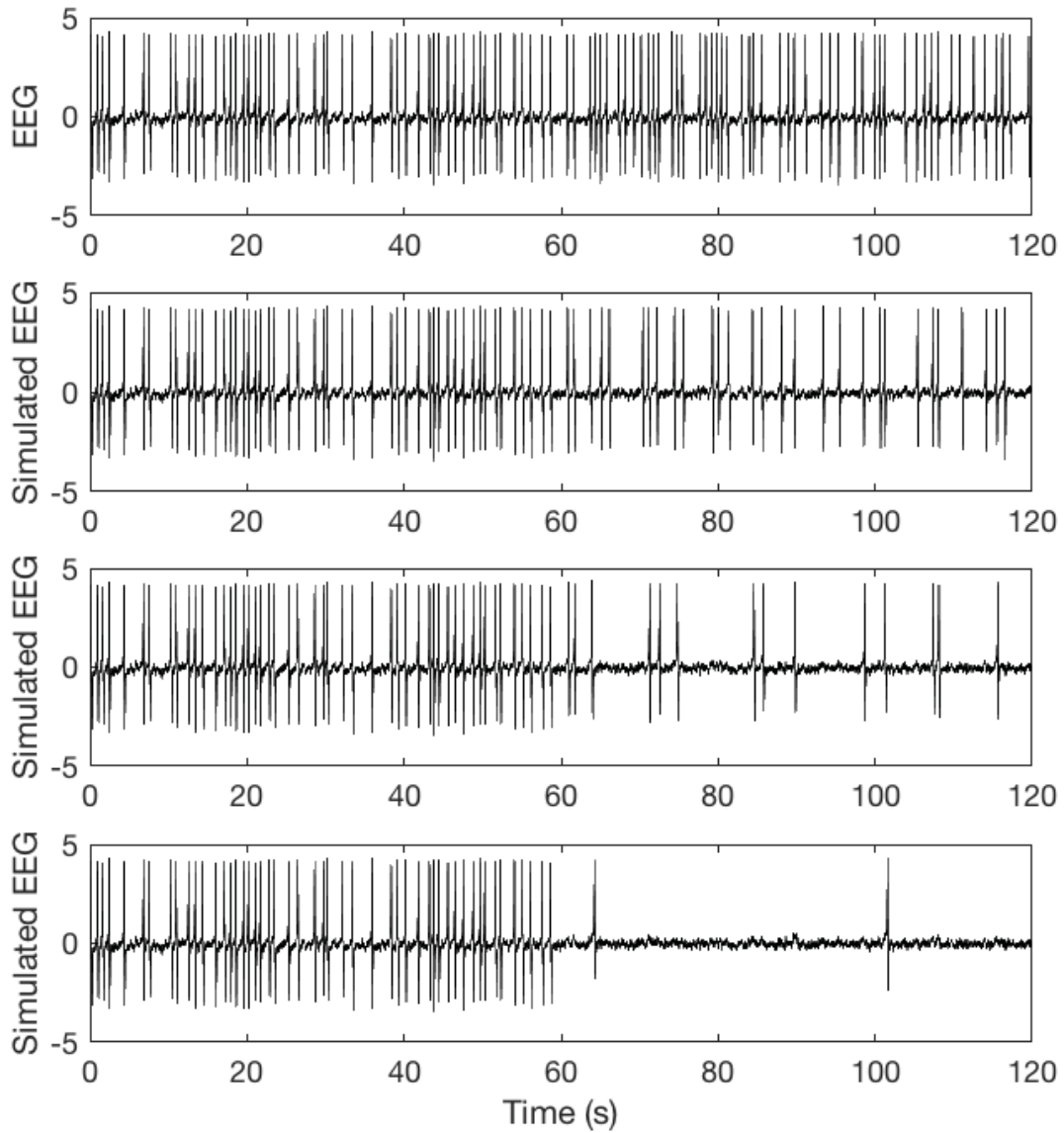


Figure 4.2: Effect of  $Q_{10,syn}$ . As  $Q_{10,syn}$  is increased from unity, frequency of epileptic discharges during cooling (60 s - 120 s) becomes less until complete termination. (From top to bottom:  $Q_{10,syn} = 1.0, 1.007, 1.013, 1.085$ .)

To model persistent discharges during cooling period, we conjecture that the reduction in the average frequency of firing caused by the first temperature

dependence should be compensated. This can be achieved through the firing response function negating the effect of  $Q_{10,syn}$  (see Discussion). A second temperature dependence is thus put forward involving a reciprocal  $Q_{10}$  factor multiplied to the average membrane potential:

$$S(v) = \frac{2e_0}{1 + e^{\left(\frac{v_{th} - Q_{10,int}^{-(T-T_0)/10} v}{\sigma_{th}}\right)}}. \quad (4.2)$$

Figure 4.1 illustrates the effect of this temperature dependence in the original firing response curve. The modified firing response curve is translated to the left and has steeper slope. In summary, two temperature parameters are introduced in this study -  $Q_{10,syn}$  and  $Q_{10,int}$ . The latter part of this study also looks at the possibility that  $Q_{10,syn}$  varies for different populations related to the differences in their respective PSP generation mechanisms.

## 4.2 Parameter estimation

Similar parameter estimation procedure was done to estimate the temperature parameters of the model from the epileptic discharge activity during cooling. The objective function involved in the estimation is modified as

$$J(\theta) = \sum E_{IDI} + E_{EffMag} + P(\theta). \quad (4.3)$$

The penalty term  $P(\theta)$  imposes the constraint that the range of discharge activity during cooling (DC) is contained within the range of the discharge activity before cooling (BC), that is, epileptic discharges are indeed suppressed during cooling:

$$P(\theta) = K ([\max\{v_{DC}\} - \max\{v_{BC}\}]_+ + [\min\{v_{BC}\} - \min\{v_{DC}\}]_+), \quad (4.4)$$

where  $[\cdot]_+ = \max\{0, \cdot\}$ ,  $\{v\}$  is the simulated discharge activity centered with respect to the baseline, and  $K$  is the strength of penalization set to 1000.

Note that a two-part estimation is performed for each experiment. The first part estimates the parameters of the Wendling et al. model (no temperature-dependent parameters) that describes the activity of epileptic discharges before

cooling. The second part estimates the temperature-dependent parameters ( $Q_{10}$  factors) during cooling using the result of the first part describing the pathological activity of the brain. Simultaneous estimation of all model parameters (before and during cooling) can be done, however, the two-part approach circumvents search issues in high-dimensional space. Furthermore, to address possible overfitting, estimation of the  $Q_{10}$  values was done using the first 40 seconds of the one-minute activity during cooling. The next 20 seconds of the activity were used for validating the model estimates from which statistical tests are performed.

## 4.3 Results

### 4.3.1 Estimation of temperature parameters

The estimation of average slow inhibitory gain and fast inhibitory gain of Wendling et al. model was aimed to reproduce epileptic discharge activity recorded from the animal model of epilepsy used. Next, we estimate the parameters involved in the temperature dependence of the model from the activity during which focal cooling is applied in the epilepsy-induced area of the brain. To assess our temperature-dependent formulation, three models were estimated from the experimental data namely: SYN (synaptic mechanism only: estimate  $Q_{10,syn}$  with  $Q_{10,int} = 1.0$ ), INT (intrinsic mechanism only: estimate  $Q_{10,int}$  with  $Q_{10,syn} = 1.0$ ), and SYN\_INT (synaptic and intrinsic mechanisms: estimate  $Q_{10,syn}$  and  $Q_{10,int}$ ). The results of the estimation were compared to no-temperature dependence (NTD) model ( $Q_{10,syn} = 1.0, Q_{10,int} = 1.0$ ). As discussed earlier, SYN captures changes in the frequency of epileptic discharges but not their magnitude (Figure 4.2). On the other hand, INT, as expected, yields estimates that are almost unity (like in the case of NTD) since the model does not have anything to compensate for having  $Q_{10,syn} = 1.0$ , i.e. no changes in average PSP yield no changes in the average firing rate.

The results suggest that temperature dependence in the post-synaptic impulse response function or firing response function alone does not capture the effect of cooling on the epileptic discharges (Figure 4.3). In fact, when both

functions have temperature dependence as formulated (SYN\_INT), we see that suppression of epileptic discharges is reproduced. Figure 4.4 shows the boxplots of the mean absolute percentage error (MAPE) of the different models from fifteen cooling experiments. Recall that the MAPE are computed from the last twenty seconds of the epileptic discharge activity during cooling which is apart from that used for the estimation (see Materials and Methods). A Wilcoxon signed rank test shows that SYN\_INT is significantly different from NTD model ( $p = 0.0034$ ).

It is also interesting to look at the estimated values of  $Q_{10, syn}$  and  $Q_{10, int}$  using SYN\_INT model (Table 4.1). We can clearly see that  $Q_{10, int}$  is only slightly less than  $Q_{10, syn}$ . This is consistent in all estimations performed from experiments on five rats. We also performed estimation of  $Q_{10}$  factors from each cooling experiment per rat where we find cases in which  $Q_{10, int}$  is slightly greater than  $Q_{10, syn}$ . These cases correspond to experiments where there are slight increases in the frequency of epileptic discharges during cooling. However, in the results that we present here,  $Q_{10}$  factors are estimated from three cooling experiments per rat which yield  $Q_{10, int}$  values that are all slightly less than  $Q_{10, syn}$ .

Table 4.1: Estimated values of  $Q_{10}$  factors from SYN\_INT model

Rat	$Q_{10, syn}$	$Q_{10, int}$
1	1.9254	1.9108
2	1.8375	1.8279
3	1.7726	1.7634
4	1.7273	1.7217
5	1.0926	1.0925

### 4.3.2 Bifurcation with respect to temperature parameters

Fixing  $Q_{10, syn}$  at 1.8, we vary  $Q_{10, int}$  from 1.0 to 2.0 at intervals of 0.01 and performed ten simulations of SYN\_INT model with different random generator seeds. We find that the magnitude and frequency of simulated activity during cooling exhibit bifurcation behavior for different temperatures (Figure 4.5). There are three apparent bifurcation regions found for cooling temperatures 15°C and

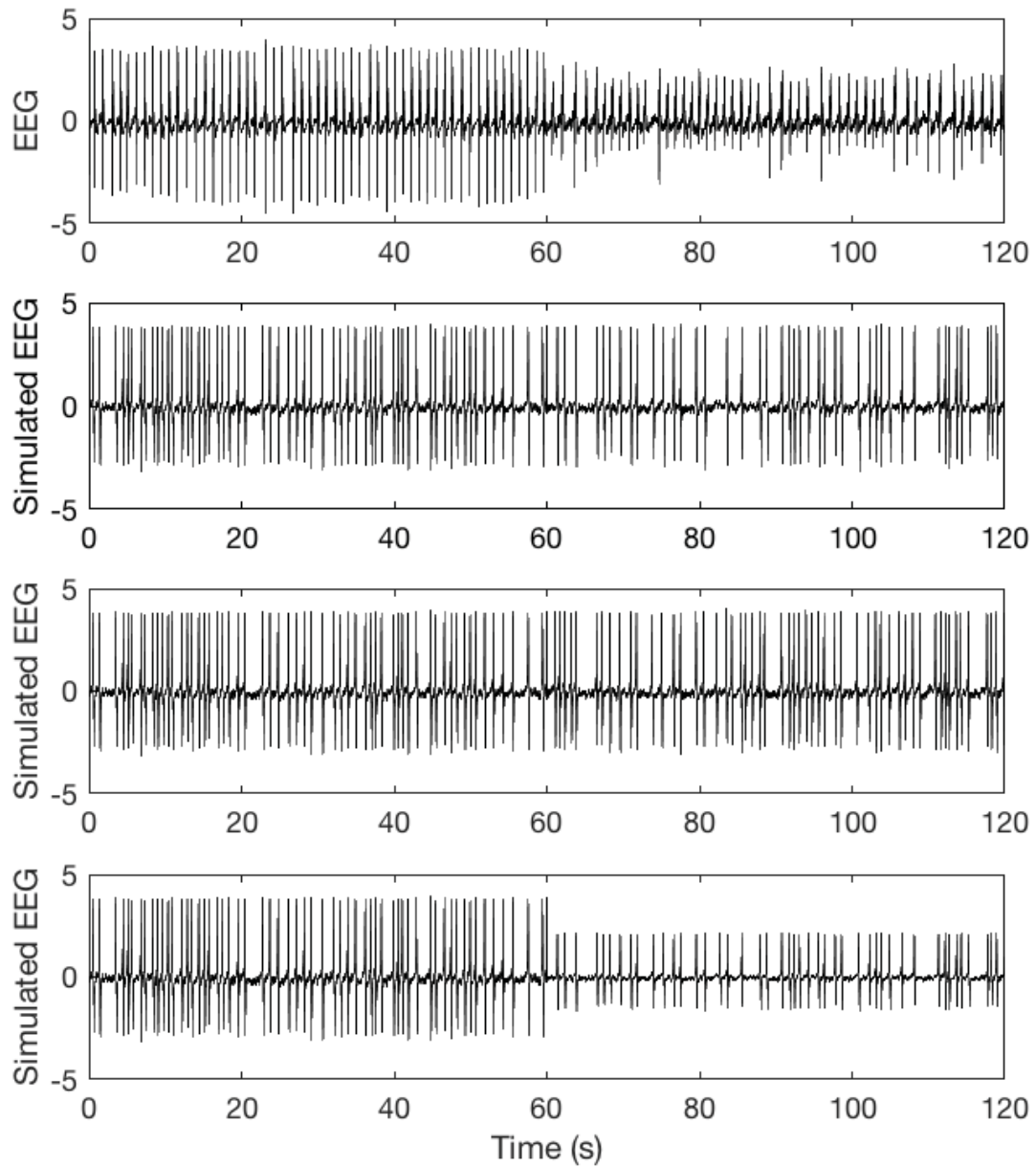


Figure 4.3: Effect of  $Q_{10,syn}$  and  $Q_{10,int}$ . Synaptic or intrinsic firing mechanism alone does not capture suppression of epileptic discharges observed in experiment. (From top to bottom: Experimental Data, SYN, INT, SYN\_INT. )

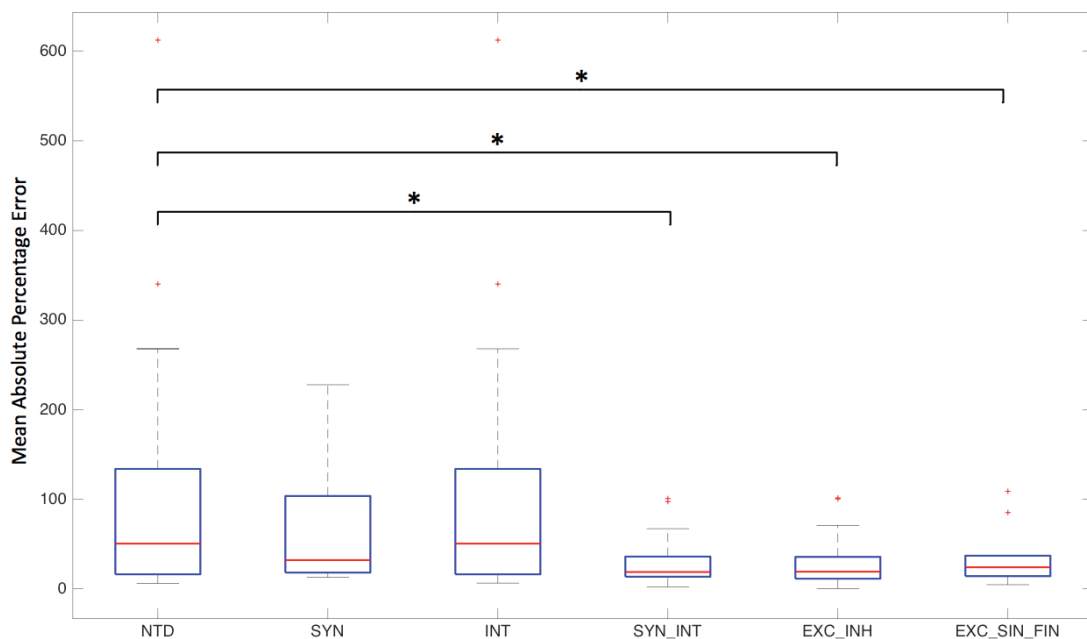


Figure 4.4: Comparison of models based on MAPE. Boxplot of MAPE of different models from experimental data. (\* $p_c < 0.05$ , Wilcoxon signed rank test with Bonferroni correction)

20°C. From baseline activity, a bistable region occurs at around  $Q_{10,int} = 1.5$  and vanishes at around  $Q_{10,int} = 1.66$  going back to baseline activity until a sudden transition to discharge activity at around  $Q_{10,int} = 1.8$  which is the same value at which  $Q_{10,syn}$  is fixed.

The results of estimation from experiments lie around the third region where  $Q_{10,int}$  values are only slightly less than  $Q_{10,syn}$  values. This region corresponds to termination of epileptic discharges or suppression of epileptic discharges to a fixed magnitude. The bistable region, on the other hand, correspond to two possible activities depending on the initial condition of the simulation- a baseline activity and an activity characterized by low-amplitude high frequency oscillations. This region, however, was not realized in the experiments. Hypothetically though, this suggests that seizure may occur with cooling when the compensatory mechanism that involves the intrinsic excitability of neurons operates with  $Q_{10,int}$  values in this region. This bistable region vanishes at weaker cooling tempera-

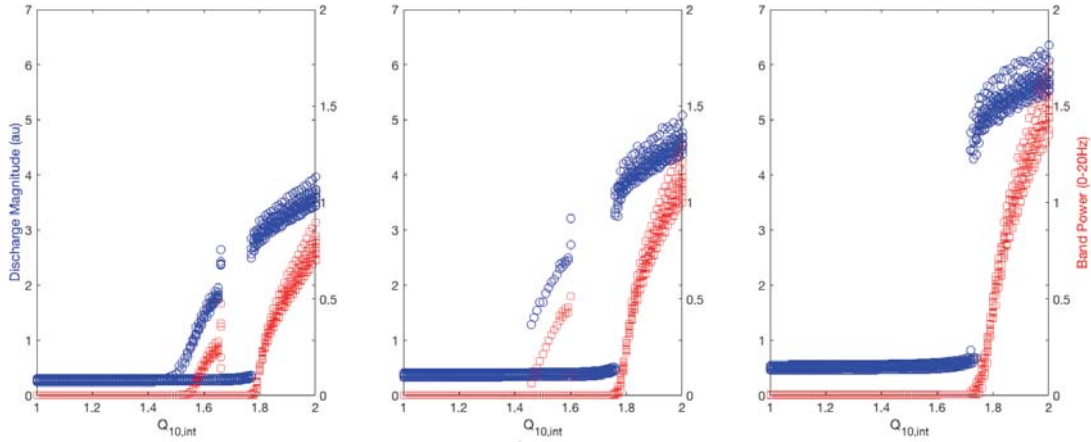


Figure 4.5: Bifurcation with respect to  $Q_{10,int}$ . With  $Q_{10,syn} = 1.8$ , magnitude and frequency of discharges exhibit bifurcation behavior with respect to  $Q_{10,int}$  at different cooling temperatures. (From left to right:  $T=15^{\circ}\text{C}$ ,  $20^{\circ}\text{C}$ ,  $25^{\circ}\text{C}$ .)

tures (Figure 4.6) indicating that such possibility of seizure may be prevented. Similar pattern of bifurcation is also observed with a bistability region that is wider at higher values of  $Q_{10,syn}$  and vanishes at lower values of  $Q_{10,syn}$  (Figure 4.6).

To gain more insight about the bifurcation behavior observed in the model, we performed a numerical continuation of the deterministic version of the model (standard deviation of input is zero) using MatCont [61]. Similarly, we fixed  $Q_{10,syn}$  at 1.8. Continuing from a fixed point with  $Q_{10,int} = 1.0$ , two saddle node bifurcations were found at around  $Q_{10,int} = 1.7996$  and  $Q_{10,int} = 1.1702$  (Figure 4.7). From the second bifurcation point, a Hopf bifurcation was found at around  $Q_{10,int} = 1.5662$  with negative first Lyapunov coefficient. This implies that a stable fixed point transitions into a stable limit cycle. These bifurcation points explain the observed bistable region in the original stochastic model above where low-amplitude high-frequency oscillations or a baseline activity can be observed depending on the initial state of the system. (Note that stationary state in the noiseless model corresponds to baseline activity in the stochastic model.) Furthermore, continuing from the Hopf bifurcation point, a limit point of cycles (LPC) is

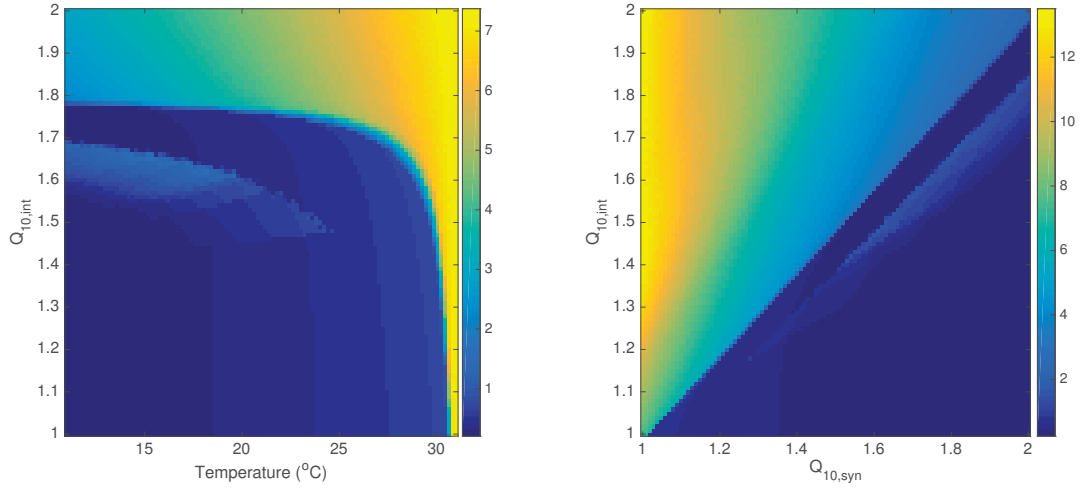


Figure 4.6: Bifurcation with respect to  $Q_{10,int}$  at different temperature and  $Q_{10,syn}$  values. Region of bistability with respect to  $Q_{10,int}$  vanishes at higher cooling temperatures (left). Similar bifurcation pattern is also observed at arbitrary  $Q_{10,syn}$  values with  $T=15^{\circ}\text{C}$  (right). The colorbars indicate discharge magnitude in arbitrary units.

found at around  $Q_{10,int} = 1.68$ . A LPC is a saddle node bifurcation for periodic orbits where two limit cycles coalesce and annihilate each other. This explains the recovery of stationary state until the first bifurcation point at which the system exits the bistable region and goes back to stable periodic orbits (discharge activity). The transition point observed in the stochastic model (termination to suppression of discharge activity) is then a sudden jump from baseline activity resulting in a magnitude of suppressed discharge activity that is proportional to the width of the hysteresis loop for a particular temperature and does not gradually increase from the magnitude of a baseline activity. At weaker cooling temperatures, such bifurcation is not observed at least in the physiologically explicable region of  $Q_{10}$  values.

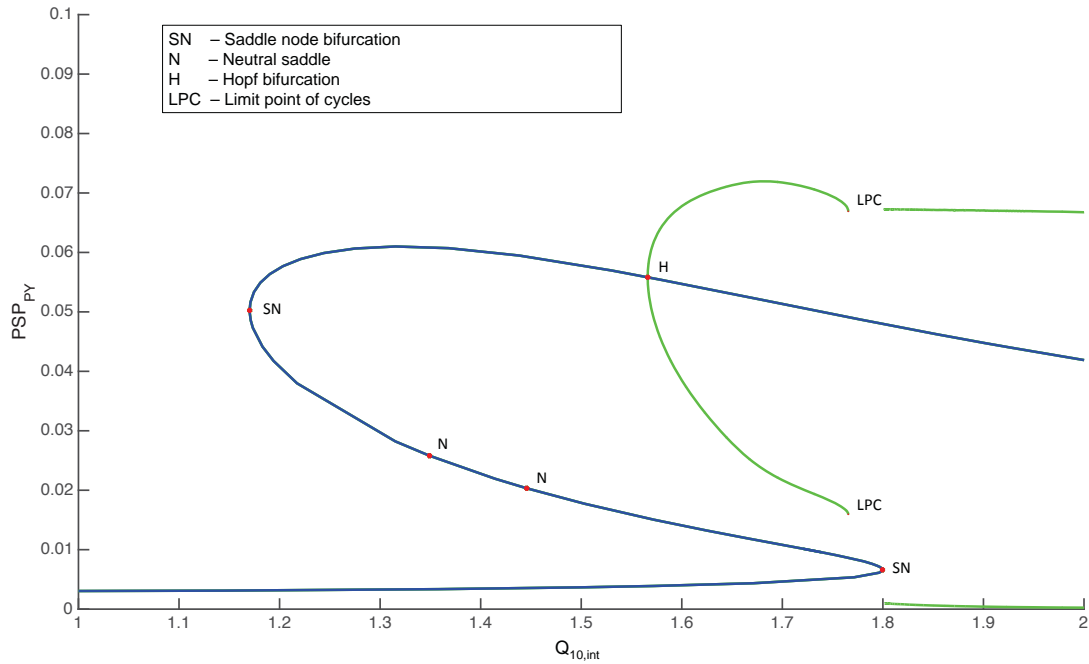


Figure 4.7: Numerical continuation of the noiseless model. Observed bifurcation patterns of discharge activity during cooling ( $T=15^{\circ}\text{C}$ ,  $Q_{10,syn} = 1.8$ ) are revealed using numerical continuation of the noiseless model. Existence of a bistable region is confirmed within which a Hopf bifurcation point is found indicating the possibility of seizure initiation at intermediate values of  $Q_{10,int}$ . A limit point of cycles inside the bistable region explains transition from stationary activity (termination of seizures) to rhythmic discharge activity corresponding to suppressed discharge activity during cooling. (Green lines indicate maximum and minimum of limit cycles.)

### 4.3.3 Differential effect of temperature on PSP generation

We also explored the possibility that cooling has differential effect on PSP generation of different neuronal populations. We investigate this by assuming that  $Q_{10,syn}$  is not homogeneous for different populations with different average synaptic gains. SYN assumes homogeneous effect of cooling across different populations. Two more models were estimated to account for the possibility of such dif-

ferential effect of cooling. In EXC\_INH, we assume differential effect of cooling on excitatory and inhibitory PSP generation involving production of glutamate and GABA respectively. In EXC\_SIN\_FIN, we further assume differential effect of cooling on slow and fast inhibitory PSP generation involving slow GABA and fast GABA respectively. Estimation of these two models were also found to yield significant difference from NTD ( $p = 0.0034$  and  $p = 0.0034$  respectively). The two models however are not significantly different from SYN\_INT ( $p > 0.01$ , Figure 4.4).

Table 4.2: Estimated values of  $Q_{10}$  factors from two other models

Model	Rat	$Q_{10,syn,EX}$	$Q_{10,syn,SIN}$	$Q_{10,syn,FIN}$	$Q_{10,int}$
EXC_INH	1	1.8056	1.8549		1.7500
	2	1.8333	1.8219		1.8333
	3	1.8333	1.7963		1.8538
	4	1.8379	1.8219		1.8461
	5	1.1667	1.1665		1.1668
EXC_SIN_FIN	1	1.7222	1.5000	1.8457	1.8333
	2	1.6111	1.8004	1.1667	1.8333
	3	1.8333	1.7597	1.9774	1.7963
	4	1.8333	1.7958	1.8774	1.8333
	5	1.1666	1.1661	1.1670	1.1667

It is interesting to note that EXC\_SIN\_FIN is able to capture termination of epileptic discharges from rat 1 under cooling temperature of  $15^{\circ}\text{C}$  which is roughly captured using SYN\_INT or EXC\_INH. Estimated  $Q_{10}$  values in Table 4.2 present some general observations. In EXC\_INH model,  $Q_{10,syn}$  values are now slightly less than  $Q_{10,syn}$  values except for rat 1 in which termination of epileptic discharges was observed. In EXC\_SIN\_FIN, higher  $Q_{10,syn,FIN}$  values were estimated especially with rats 3 and 4. On the other hand, lower  $Q_{10,syn,EX}$  values were observed for rats 1 and 2 in which termination of epileptic discharges were found while lower  $Q_{10,syn,SIN}$  values for rats 3 and 4 in which epileptic discharges are only suppressed during cooling. These observations suggest that termination

or suppression of epileptic discharges can result from different synaptic responses of different neuronal populations to cooling. Figure 4.8 and Figure 4.9 show how the different models reproduce termination or suppression of epileptic discharges in rats 4 and 1, respectively.

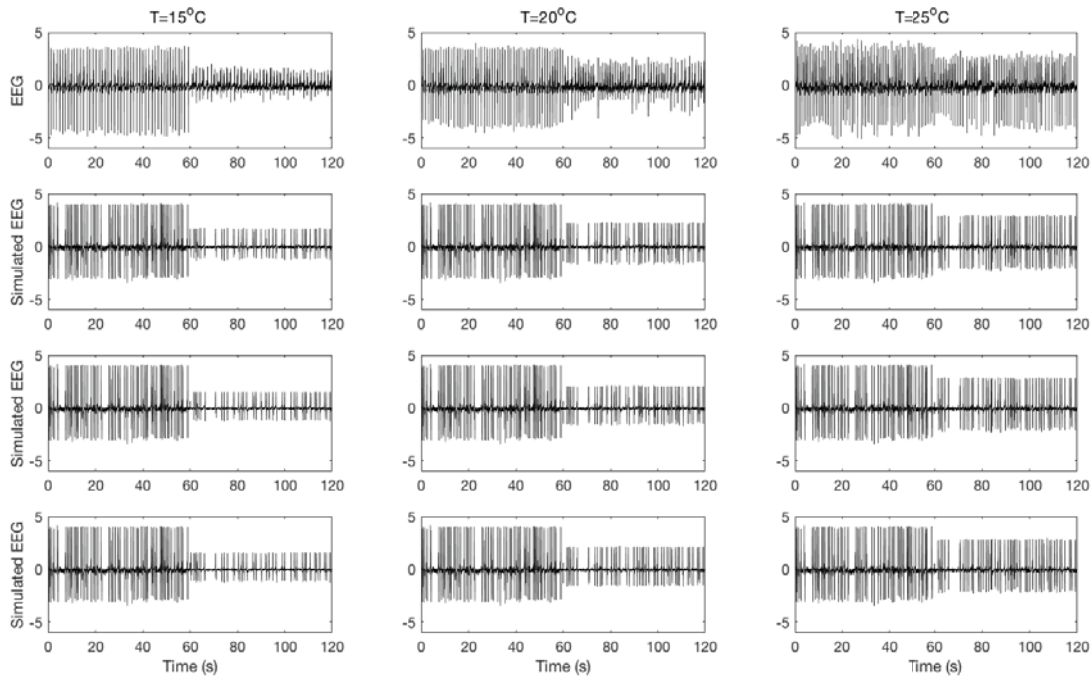


Figure 4.8: Simulated activity from rat 4. Suppression of epileptic discharges are replicated by the different models. (From top to bottom: Experimental data, SYN\_INT, EXC\_INH, EXC\_SIN\_FIN)

Finally, it can also be observed that the estimated  $Q_{10}$  values are between 1.7 and 2.0 except those estimated from rat 5 in which case the estimated values are less than 1.2. The estimation result from rat 5 can be substantiated by observing the activities during cooling of rat 5 at different temperatures showing less evidence of suppression of epileptic discharges (Figure 2.2).

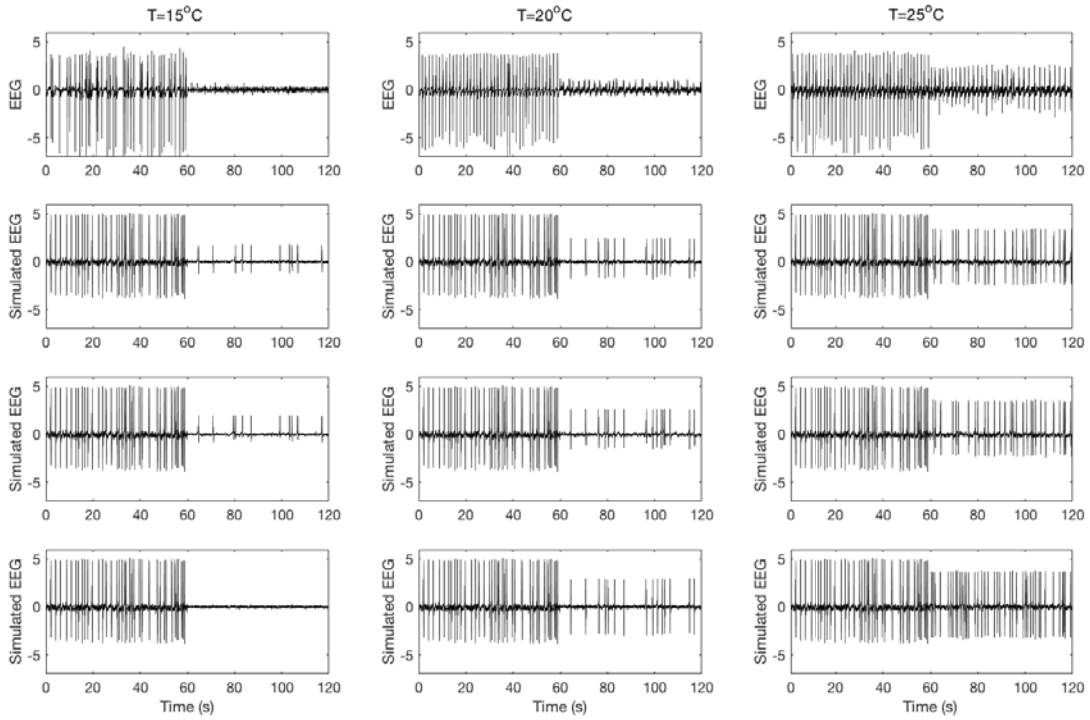


Figure 4.9: Simulated activity from rat 1. Termination of epileptic discharges at cooling temperature of  $15^{\circ}\text{C}$  is captured by model 5 . (From top to bottom: Experimental data, SYN\_INT, EXC\_INH, EXC\_SIN\_FIN)

## 4.4 Discussion

Neurotransmitters play a central role in the generation of PSP [62]. They are released in response to  $\text{Ca}^{2+}$  influx after depolarization of pre-synaptic terminal and bind to their receptor molecules at the post-synaptic membrane, opening or closing ion channels, and thereby generate excitatory or inhibitory PSP. It has long before suggested that neurotransmitter release has temperature dependence which causes changes in PSP generation [63]. This was confirmed by experimental observations of reduced efficacy of neurotransmitter vesicle release and reduced extracellular glutamate concentration during cooling [39,41] that imply lower neurotransmitter concentration at the synapses to bind at the post-synaptic receptor and generate PSP. In light of this, it was straightforward to assume a tempera-

ture dependence on the post-synaptic impulse response function in a neural mass model of the population activity'. Similar to temperature-dependent formulation of Hodgkin-Huxley type neurons [64–66], temperature dependence in Wendling et al. model is modelled using a temperature coefficient given by a  $Q_{10}$  factor. This factor accounts for mean-field effect of temperature to several processes occurring during PSP generation across the neuronal population. For example, diffusion of neurotransmitters,  $Ca^{2+}$ , and receptor proteins [67–69] are slowed down at different rates at decreasing temperatures affecting efficacy of neurotransmitter vesicle release and the binding of neurotransmitters at the post-synaptic terminal receptors which regulate the activities of specific ion channels. Simply,  $Q_{10, syn}$  is added to the post-synaptic impulse response function and can be interpreted as direct attenuation of the average post-synaptic gain of the population or synaptic conductance of one neuron. This yields lower average PSP values when temperature is decreased from a baseline temperature. This decreases or increases the average membrane potential of the populations to which the population provides excitation or inhibition respectively. Reduced average membrane potential yields lower frequency of firing. In fact, we saw that termination of epileptic discharges results when the firing frequency approaches zero with  $Q_{10, syn} \approx 1.085$  but with nonsignificant decrease in the magnitude of isolated discharges. In contrast, what was actually observed from experiments is that epileptic discharges were persistent during cooling but suppressed in magnitude. This is not reproduced by the model because of the nonlinearity of the firing response function. A  $Q_{10}$  value of 1.085 does not significantly suppress the magnitude of discharges but its effect on attenuated PSP responses significantly reduces the firing activity of the receiving population. Interestingly, in some cases in the experiment, slight increases in frequency of epileptic discharges were observed (Figure 2.2). These lead us to assume that a concomitant mechanism plays a role during cooling which may involve the intrinsic excitability mechanism of neurons compensating for the effect of reduced PSP on the average firing activity of the populations. Thus, a reciprocal  $Q_{10}$  factor was formulated as put forward in Eq. (4.2). Similarly, the  $Q_{10}$  factor involved here accounts for mean-field effect of temperature to several processes occurring during action potential generation such as diffusion of ions and temperature effects on ion channel gating across the neuronal population.

Figure 4.1 shows how the average firing rate is compensated by the second temperature dependence. The firing frequency of a positive average membrane potential in the original firing response curve corresponds to an increased firing frequency at the same value of average membrane potential in the temperature dependent curve. The effect is opposite for negative average membrane potentials and rather minimal. A direct physiological interpretation of this mechanism can be examined if we write the equation in its equivalent form

$$S(v) = \frac{2e_0}{1 + e^{\left( \frac{Q_{10,int}^{(T-T_0)/10} v_{th} - v}{Q_{10,int}^{(T-T_0)/10} \sigma_{th}} \right)}}, \quad (4.5)$$

where the  $Q_{10}$  factors are now with the parameters  $v_{th}$  and  $\sigma_{th}$ . Recall that  $v_{th}$  is the average threshold of firing of neurons and  $\sigma_{th}$  is the variability in the thresholds of excitation of neurons. This then implies that as a compensatory mechanism, cooling lowers both the average and variance of the distribution of the firing thresholds of neurons in the population. Hence, even if the average PSP is reduced resulting in lower average membrane potential, epileptic discharges can still be persistent since lower average threshold of firing allows for subthreshold activity before cooling to become suprathreshold during cooling. This can be seen as a form of homeostasis in the firing activity of the neuronal population involving both synaptic and intrinsic excitability mechanisms. Surprisingly, the combined mechanisms result in suppression of epileptic discharges in terms of magnitude which is not captured if we assume temperature dependence in the post-synaptic impulse response function alone. This is because higher  $Q_{10,syn}$  values now significantly reduce PSP responses (Figure 4.7(b)) but the effect of which is compensated by the reciprocal of  $Q_{10,int}$ . Slight increase in frequency of discharges observed in the some of the experiments can be realized if  $Q_{10,int}$  is made slightly greater than  $Q_{10,syn}$ . Further increasing  $Q_{10,int}$  proportionately increases the frequency of discharge activity (Figure 4.5).

Reduced threshold potential of firing during cooling has been reported on an early experiment with squid axons [28]. Experiments with mammalian brains [29, 70, 71] reported that cooling depolarizes cell membrane potential and

increases input resistance. In [71], Volgushev et al. noted that cooling-induced depolarization of cell membrane occurs with an even higher gradient giving a marked decrease in the difference between the spiking threshold and the actual resting membrane potential. Thus, cooling brings the cells closer to spiking threshold, increasing excitability and decreasing variability in excitation levels across neuronal population. They proposed that such cooling-induced depolarization of the cell membrane may be attributed mainly by reduction of partial  $K^+$  conductance. Variability in threshold potential of firing has also been reported to increase with recent spiking activity [72]. We suppose that the opposite happens during cooling. As discussed earlier, cooling can decrease average firing rate of neurons which can imply less recent spiking activity. Henze and Buzsaki [72] suggested that prior action potentials cause  $Na^+$  channel inactivation that recovers with approximately a one-second time constant, increasing action potential threshold during this period. On the other hand, a study by Yu et al. [73] suggests that firing threshold variability can be explained by backpropagation of action potentials. Moreover, cooling was shown to strongly inhibit A-type  $K^+$  channels in DRG neurons [74] while these channels are reported to regulate action potential backpropagation in CA1 pyramidal neurons [75]. This might be in conflict with our finding that cooling reduces variability in firing thresholds since inhibited A-type  $K^+$  channels enhance backpropagating action potentials which in turn increases variability in firing thresholds. Then again, it is also possible that a net decrease in action potential backpropagation results as cooling can attenuate other critical factors such as density of  $Na^+$  at axon initial segment [76] and ion transport at nodes of Ranvier [77].

Estimation of the model from cooling experiments indicated that the  $Q_{10}$  factor for the firing response function is only slightly less than the  $Q_{10}$  factor for the post-synaptic impulse response function. This means that during cooling, the intrinsic excitability mechanisms of neurons just balance out the effect of temperature change on PSP generation. At first, it seemed that when  $Q_{10,int} \approx Q_{10,syn}$ , discharge activity is suppressed but not terminated and when  $Q_{10,int}$  is strictly less than  $Q_{10,syn}$ , discharge activity is terminated. To verify this generalization, we simulated the model for different values of  $Q_{10,int}$  fixing  $Q_{10,syn} = 1.8$ . This led

us to discover bifurcation patterns in the model which were confirmed using numerical continuation on the noiseless version of the model. First, we have verified that when  $Q_{10,int} \approx Q_{10,syn}$ , discharge activity is suppressed but not terminated. At this point, the intrinsic mechanism just "fully" compensates the effect of the synaptic mechanism resulting to a discharge activity that has approximately the same frequency but reduced in magnitude. However, we found out that when  $Q_{10,int} \lesssim Q_{10,syn}$ , discharge activity is terminated only up to a certain value of  $Q_{10,int}$  and a high-frequency seizure activity can arise with a wide range of intermediate  $Q_{10,int}$  values. As far as we are knowledgeable, there has been no report that seizure activity was ever observed in focal cooling of epileptic discharges. Moreover,  $Q_{10,int}$  values are not interpretable in terms of how intrinsic firing mechanisms can give rise to such values which would allow experiments to verify such finding. In theory, this should guide the design of implantable cooling devices which would necessitate a feedback control law to terminate cooling or use weaker cooling temperature when a possible seizure can arise. Figure 4.10 indicates that both the pyramidal cell population and the interneuronal populations exhibit the same activity resulting in either seizure activity or suppressed discharge activity depending on  $Q_{10,int}$  and initial conditions. Similar bifurcation patterns were observed for arbitrary values of  $Q_{10,syn}$  other than 1.8. Our estimation results indicated  $Q_{10}$  values around 1.8 which was, surprisingly, also reported in previous studies involving voltage-gated  $\text{Na}^+$  channel (VGNC) dynamics [14]. Then again, *in vitro* studies [71, 78] suggest that involvement of VGNC might be ruled out as abortion of epileptiform discharges were seen to be associated with a depolarization block. Perfect depolarization is against changes in the gating property of  $\text{Na}^+$  channels as initially hypothesized, i.e., cooling is not inducing a liquid phase transition in phospholipid bilayer of the membrane thereby distorting the channel's property, rather through other mechanisms.

Another interesting study by Motamedi et al. [78] with an *in vitro* epilepsy model showed that cooling has differential effect on the firing rates of pyramidal cells and interneurons. This actually motivated the models where we included more temperature dependent parameters to investigate possible differential effect of cooling on PSP generation. This relies on the assumption that cooling may have

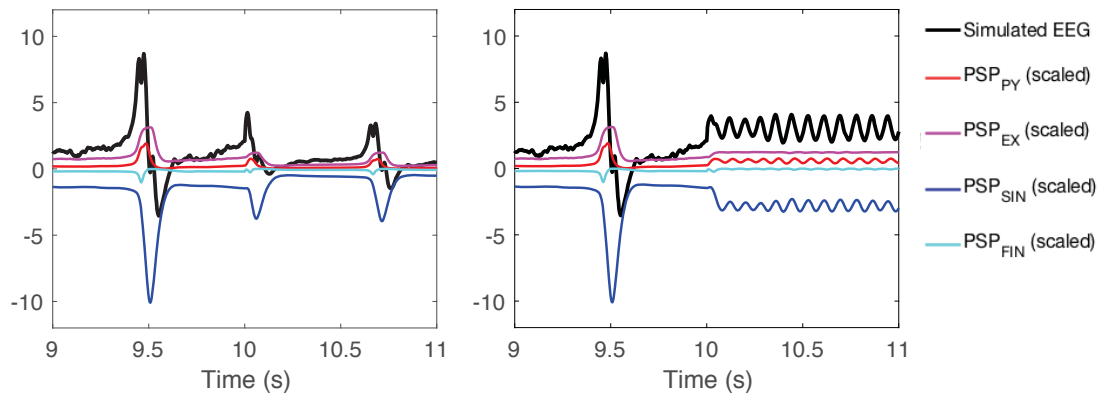


Figure 4.10: Contribution of population activity to LFP at different  $Q_{10,int}$ . (Left) PSP inputs from pyramidal cells and interneurons are attenuated resulting to suppression of discharge activity during cooling. (Right) PSP inputs from pyramidal cells and interneurons exhibit low amplitude rhythmic activity contributing to initiation of seizure activity.

differential effect on different neurotransmitters responsible for generating PSP. However, in this study, the model parameters were estimated from *in vivo* EEG recordings which have clear departures from the aforementioned *in vitro* study. We can speculate though that it may be possible to reproduce such differential effect of cooling on the activity of pyramidal cells and inhibitory interneurons if we had isolated EEG recordings from pyramidal cell population and interneuronal population activities and from which we could estimate the model parameters with an appropriate modification of the objective function (Eq. (4.3)). Nevertheless, when the effect of cooling on inhibitory interneurons is much less than on excitatory interneurons, reduced average membrane potential of pyramidal cell population results and consequently, reduction in the average firing frequency of the population is observed as reported in the study.

The results presented in this paper only considered the steady-state effect and does not include transient dynamics of cooling on epileptic discharges although some experiments have noted the effect of rate of cooling on termination of epileptic discharges. For instance, an *in vitro* study [45] reported that during slow cooling, epileptic discharges persist with decreasing amplitude un-

til termination is achieved with further temperature drop. In contrast, rapid cooling achieves immediate termination of the discharges. The gradual decrease in amplitude of epileptic discharges during slow cooling can be captured by the model using an appropriate model for temperature dynamics (e.g. Newton's Law of Cooling). In its present form, immediate termination of discharges by rapid cooling can be explained by our model as a case where  $Q_{10,int} \lesssim Q_{10,syn}$ , i.e. reduction in average and variance of firing thresholds across neuronal population is not able to compensate reduction in discharge frequency due to reduced average membrane potential resulting from attenuation of post-synaptic activity. Alternatively, such transient effect may be modelled by a  $Q_{10}$  dynamics that decays from a non-steady state value to a steady state value proportional to the rate of cooling. In most *in vitro* studies that we reviewed, steady-state termination of epileptic discharges was achieved using either slow or rapid cooling down to a constant temperature. In contrast, termination may not be always possible in *in vivo* setting. We surmise that the compensatory mechanism put forward by the model is more concomitant in *in vivo* than in *in vitro* environment.

# 5 Focal brain cooling for secondary generalized epilepsy

In the previous chapter, we considered the case in which focal cooling is applied to the region of an animal brain induced with seizure. In real situations, however, seizure activity can propagate from one region of the brain, which is usually pathologic, to nearby and possibly distant regions of the brain. This is the case for secondary generalized epilepsy (SGE) or the generalization of partial epilepsy. To address whether or not thermal neuromodulation is effective in this setting, it is necessary to first simulate how brain activity propagates from one brain region to another. In the following sections, we review earlier coupled neural mass models and present the problem of dimensional inconsistency or physiological interpretability of the model. We then propose a coupling model that has both dimensionally consistency and physiological interpretability, and investigate the parameters of the model with which we can simulate propagation of seizure activity. Thence, we simulate cooling of the pathologic region of the brain and find out whether it is effective against the spreading of seizure activity.

## 5.1 Problem overview

Recent studies are trying to establish that epilepsy is a network disease; that is, surgical removal of the pathologic area of the brain in medically-intractable epilepsy patients may not be sufficient to guarantee remission. Using a phenomenological model of brain activity, Petkov and colleagues put forward that the network has a critical role in brain ictogenesis or the ability to initiate seizure activity [79–81]. Hebbink et al. [82] illustrated using simulations of the

same model, that the removal of the pathologic brain region, in most cases, is not the best approach to reduce frequency of seizure activity. Goodfellow et al. [83] utilized a physiological model based from the earlier work of Wendling et al. [84] and proposed an ictogenecity index that quantifies the contribution of one brain region in a network of brain regions to seizure activity. The coupling model, which was originally proposed by Jansen and Rit [34], involves a constant gain function that could however lack direct physiological interpretability. Recently, Lopes et al. [85] used a different coupling model proposed by Goodfellow et al. [86] with the same underlying neural mass model in [83] to identify optimal resection sites for surgical treatment. The coupling model, however, dismisses the originally proposed mechanism that brain activity is propagated to a connected brain region via a different post-synaptic impulse response function with slower synaptic time constant. This begs the question of which between the two coupling models is more appropriate to use. This could be crucial in understanding precise mechanisms of seizure activity initiation and propagation.

We propose a coupled neural mass model reconciling the existing two coupling schemes. Moreover, the coupling parameter can be interpreted as strength of synaptic connectivity between primary cell populations from two brain regions. This can translate to new synapses formed via axonal sprouting [87, 88] or enhancement of functional connectivity [89] between two brain regions. We show that the strength of coupling determines whether a seizure activity can initiate in one brain region and propagate to connected brain regions. This offers a parsimonious yet physiological model that can generate a network of brain regions that participate in the initiation and propagation of seizure activity in the brain. Using sophisticated technologies such as advanced diffusion magnetic resonance imaging [90, 91] that can resolve the strength of structural connections between brain regions, the coupling model can be used for pre-surgical diagnosis of medically-intractable patients to identify optimal sites for resection. In this study, we investigate the feasibility of focal brain cooling as an alternative therapeutic treatment for secondary generalized epilepsy cases.

## 5.2 Review of coupled neural mass models

One of earliest model for coupled neural masses was introduced by Jansen and Rit to investigate visual evoked potentials [34]. In the model, two neural masses, simulating the visual cortex and prefrontal cortex, are coupled together. The double column model was extended by Wendling et al. to multiple brain regions to analyze epileptic intracranial EEG signals. The model has been adopted in several including recent studies on propagation of seizure activity in brain networks [83, 92].

The coupled neural mass model involves an average post-synaptic potential from the afferent neural mass  $i$  that is multiplied by a coupling parameter  $K_{ij}$  and is added to the subcortical input to the receiving neural mass  $j$ . In detail, the post-synaptic impulse response function  $h_d(t)$  for the propagated signal between the coupled neural masses was assumed to involve a time constant  $1/g_d$  that is slower than that of between populations within the same neural mass:

$$h_d(t) = G_d g_d t e^{-g_d t}; t \geq 0. \quad (5.1)$$

The propagated average post-synaptic potential from the afferent neural mass  $i$  is given by

$$v_d^{(i)}(t) = h_d(t) * S(V_{PY}^{(i)}) \quad (5.2)$$

where  $V_{PY}^{(i)}$  is the average membrane potential of the pyramidal cell population of neural mass  $i$ , and  $S(\cdot)$  is the firing response function in Eq. 3.1. This is then added as an input to an receiving neural mass  $j$ , contributing to the excitatory post-synaptic potential as

$$v_{EX}^{(j)}(t) = h_{EX}(t) * \left( S(V_{EX}^{(j)}) + \frac{1}{C_{EX \rightarrow PY}} \left( u_N(t) + \sum_i K_{ij} v_d^{(i)}(t) \right) \right) \quad (5.3)$$

where  $u_N(t)$  is a noisy subcortical input and  $V_{EX}^{(j)}$  is the average membrane potential of the excitatory interneuron of neural mass  $j$ . Note that the factor  $\frac{1}{C_{EX \rightarrow PY}}$  is due to the fact that the average membrane potential of the pyramidal cell population is computed as:

$$V_{PY}^{(j)}(t) = C_{EX \rightarrow PY} v_{EX}^{(j)} - C_{SIN \rightarrow PY} v_{SIN}^{(j)} - C_{FIN \rightarrow PY} v_{FIN}^{(j)}. \quad (5.4)$$

Inspecting Eq. (5.3), we can say that the model has dimensional inconsistency if the coupling parameter were taken as a dimensionless quantity since the first two terms in the input are both in terms of firing rate while  $v_d^{(i)}(t)$  is a potential term. Otherwise,  $K_{ij}$  represents a constant gain function that converts the propagated potential to firing frequency, which may not be physiologically interpretable. In fact, Goodfellow et al. [86] proposed a dimensionally consistent model as follows:

$$v_{EX}^{(j)}(t) = h_{EX}(t) * \left( S(V_{EX}^{(j)}) + \frac{1}{C_{EX \rightarrow PY}} \left( u_N(t) + \sum_i K_{ij} S(V_{PY}^{(i)}(t)) \right) \right). \quad (5.5)$$

The model, however, altogether dismisses the proposed mechanism by the former that the propagation of brain activity to a connected neural mass involves a different impulse response function with slower average synaptic time constant. Since  $h_{EX}(t) = h_{PY}(t)$ , Eq. (5.5) is equivalent to

$$V_{PY}^{(j)}(t) = C_{EX \rightarrow PY} v_{EX}^{(j)} - C_{SIN \rightarrow PY} v_{SIN}^{(j)} - C_{FIN \rightarrow PY} v_{FIN}^{(j)} + \sum_i K_{ij} v_{PY}^{(i)}(t). \quad (5.6)$$

separating the excitatory contribution of afferent neural masses from that of within the neural mass (excitatory interneurons and subcortical input).

### 5.3 Proposed coupled neural mass model

For the reason discussed in the previous section, we propose a coupled neural mass model that has both dimensional consistency and direct physiological interpretability of the coupling parameter. We retain the important aspect of the coupling model by Jansen and Rit regarding the propagation mechanism that involves a different impulse response function with slower average synaptic time constant and possibly different average synaptic gain as in Eq. (5.1). This is then used to modify the equivalent coupling model by Goodfellow et al. (Eq. (5.6)). Specifically, the proposed model puts forward that the propagated post-synaptic potentials from the afferent neural masses contribute to the local field potential

of the receiving neural mass. The coupling term is then given by:

$$V_{PY}^{(j)}(t) = C_{EX \rightarrow PY} v_{EX}^{(j)} - C_{SIN \rightarrow PY} v_{SIN}^{(j)} - C_{FIN \rightarrow PY} v_{FIN}^{(j)} + \sum_i K_{ij} v_d^{(i)}(t). \quad (5.7)$$

The first three terms are synaptic contributions from excitatory and inhibitory interneurons within the neural mass and the last term sums all propagated post-synaptic input from afferent neural masses. Clearly, the model is dimensionally consistent since all terms involved are potential terms. Moreover, the coupling parameter  $K_{ij}$  can now be interpreted in the same way as  $C_{PY \rightarrow EX}$ , in particular, it is the average number of synaptic connections between the pyramidal cell populations of the coupled neural masses.

## 5.4 Results

### 5.4.1 Coupling gives rise to seizure activity

We investigate the parameters of the proposed coupling model and how changing them can give rise to different kinds of seizure activity. In the original model of Jansen and Rit [34], the authors stated that the average synaptic time constant involved in the propagated activity between neural masses is slower than within a neural mass and proposed  $g_{PY} \approx g_{PY}/3$  without further justification. We simulated the model with varying values of  $g_d$  and  $K$  ( $K_{ij} = K_{ji}$ ) for two neural masses that demonstrate normal activity ( $G_{SIN} = 50$ ) when not coupled together. In Figure 5.1, we show a map of the amplitude and band powers of simulated activity of the coupled neural masses with respect to the varied parameters. We can observe that seizure can arise when the neural masses are coupled together for a range of  $K$  values that increases with increasing value of  $g_d$ . Interestingly, we find that at around  $g_d = 0.33g_{PY}$ , different types of seizure activities are demonstrated with increasing  $K$  as evident from powers of theta, alpha, and beta-gamma bands. A simulation of these activities is shown Figure 5.2.

Notably, a minimum value of  $K$  is needed before a discharge activity emerges. We suppose that this is the strength of coupling required that could alter

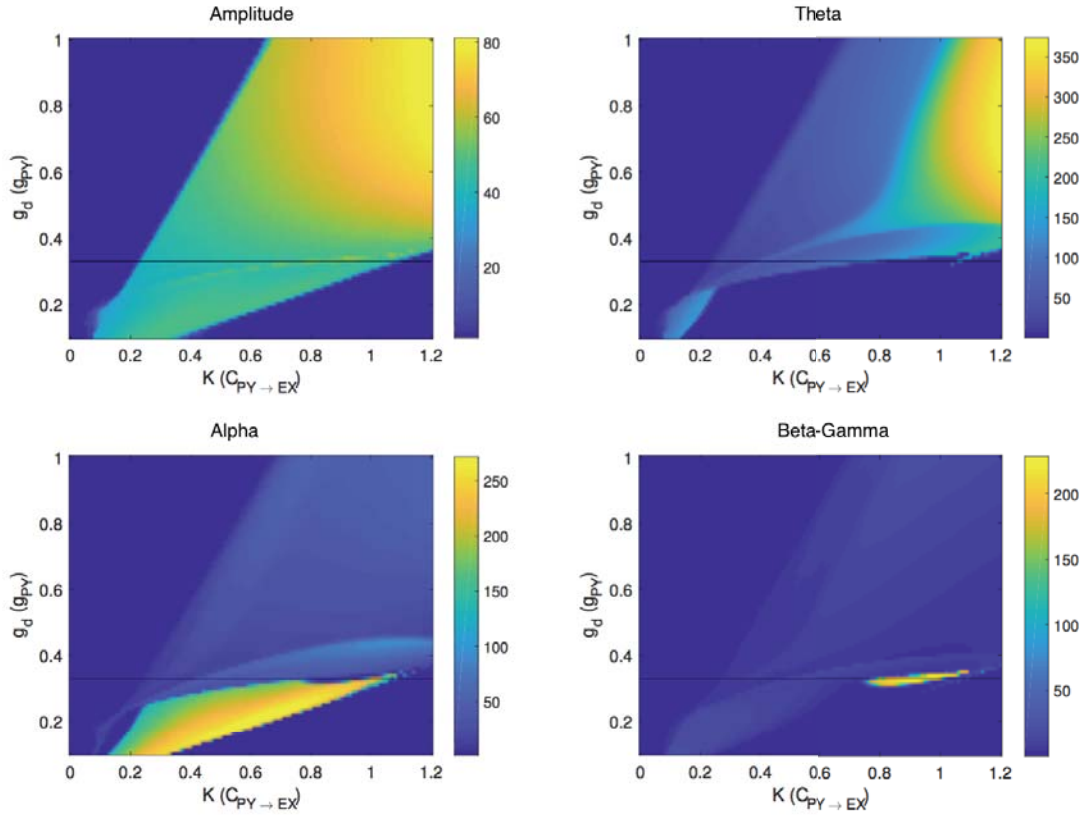


Figure 5.1: Activity map from reciprocally coupled neural masses with varying values of  $g_d$  and  $K$ . Different kinds of seizure activity are observed at around  $g_d = 0.33g_{PY}$  characterized by band powers with increasing values of coupling parameter.

the excitation-inhibition balance by increasing excitatory contribution to the local field potential and consequently would give rise to seizure activity even when the neural masses are intrinsically non-pathological. Increasing this coupling strength increases the degree of pathology in terms of frequency of discharges, developing into high-frequency periodic oscillations. Upon further increases in  $K$ , this oscillatory activity decreases in amplitude, higher frequency components are removed, then waxes and wanes; after a maximum value of  $K$ , the neural masses no longer demonstrate seizure activity; rather high theta activity is exhibited with higher baseline value (Figure 5.3). On the other hand, if the initially uncoupled neural

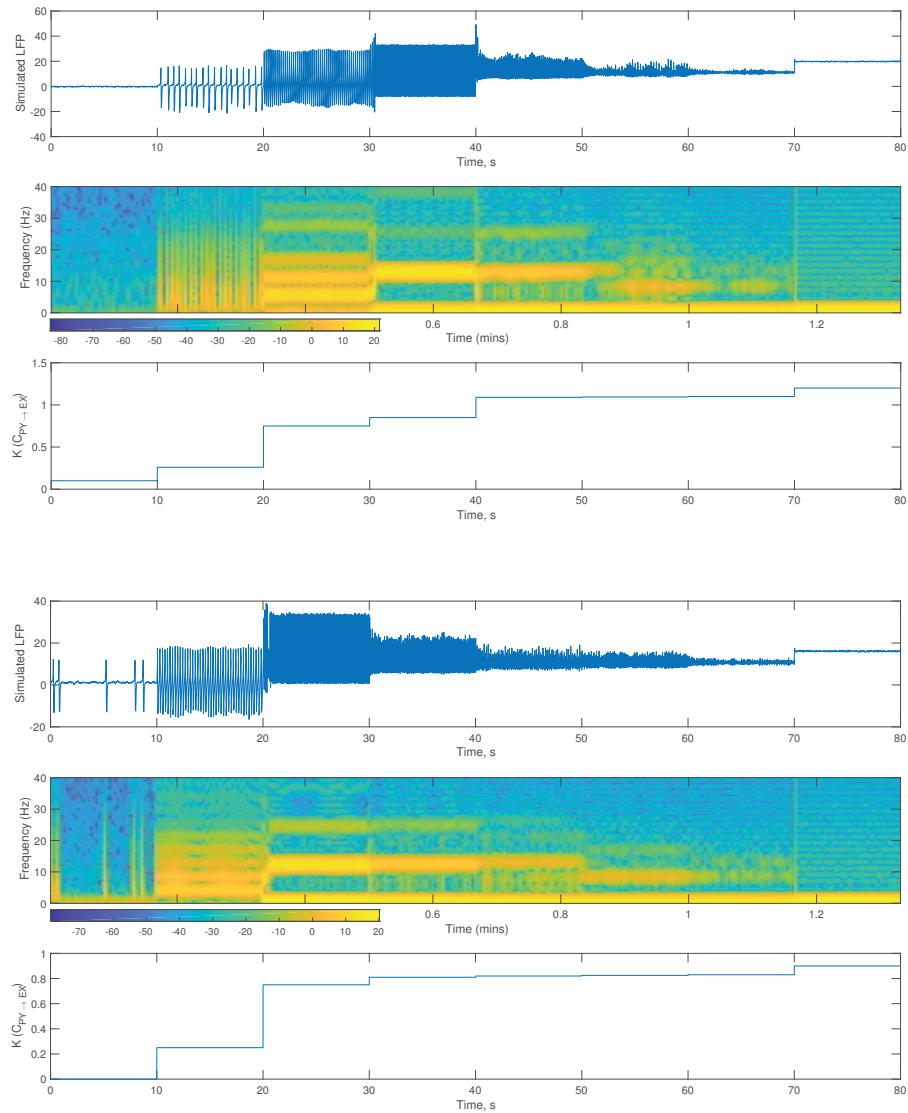


Figure 5.2: Simulated activity of coupled neural masses with increasing values of  $K$ . Initially uncoupled neural masses are non-pathological ( $G_{SIN} = 50$ ) and pathological ( $G_{SIN} = 40$ ) in top and bottom plots respectively.

masses already demonstrate pathological activity ( $G_{SIN} \leq 40$ ) such as epileptic discharges, coupling them only results to increased level of pathology but exhibit similar evolution to different kinds of seizure activity as the strength of coupling

between them is increased until a maximum coupling strength is reached after which seizure activity ceases.

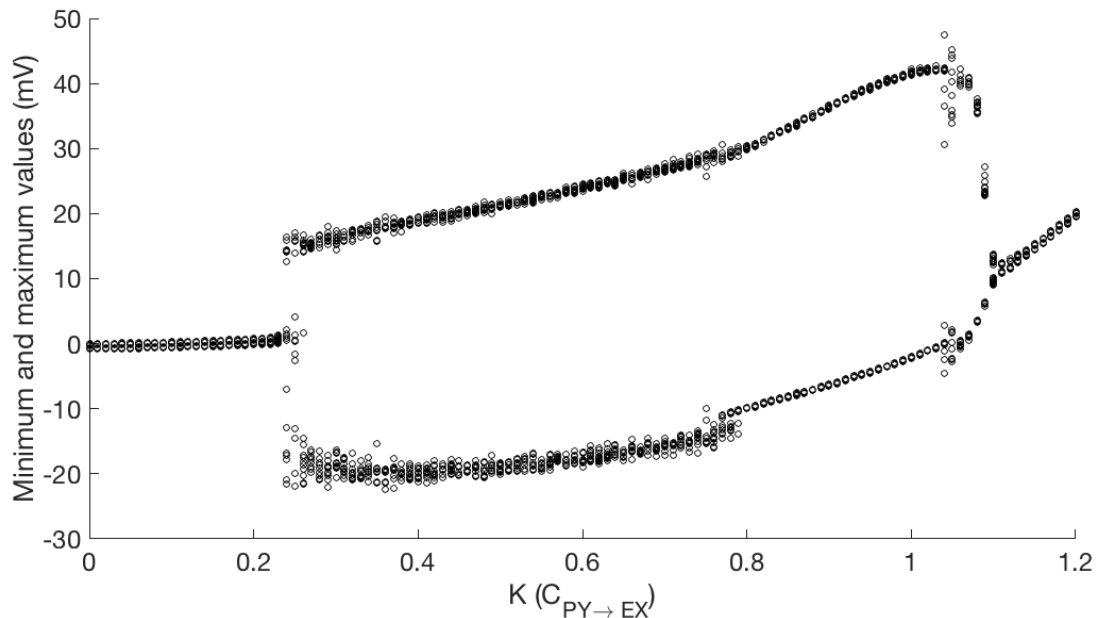


Figure 5.3: Seizure activity with respect to  $K$ . Ten simulation runs for two reciprocally coupled neural masses at different coupling strengths.

### 5.4.2 Effective coupling from multiple afferents

In real brain networks, one brain region may be coupled with several other brain regions. It is then interesting to look at the case where a neural mass is coupled with multiple afferent neural masses and define an effective coupling strength as the sum of coupling strengths from all afferent neural masses. We then ask whether this situation requires the same minimum effective coupling strength for seizure activity to emerge. To answer this, we simulated one neural mass that is reciprocally coupled with  $N$  afferent neural masses, each with coupling strength  $K$ . The effective coupling strength is then  $NK$ . In Figure 5.4, we can observe that the minimum effective coupling strength needed to initiate seizure activity increases and approaches a threshold as the number of afferent neural masses is

increased. For example, a neural mass that is reciprocally coupled with four neural masses requires  $\approx 0.4C_{PY \rightarrow EX}$  in total to initiate seizure activity compared to  $\approx 0.24C_{PY \rightarrow EX}$  with just one neural mass. This can indicate desynchronization between the excitatory contributions of the afferent neural masses that are each reciprocally coupled to the same neural mass.

We also simulated the case in which the coupling of a neural mass with multiple afferent neural masses is unidirectional as shown in Figure 5.4. Initiation of seizure activity on the receiving neural mass requires greater effective coupling strength around  $0.6C_{PY \rightarrow EX}$  regardless of the number of afferents that individually demonstrate normal activity. This suggests that reciprocal coupling lowers the required effective coupling strength to initiate seizure activity by enhancement of recurrent excitation. We suppose that if the afferent neural masses themselves are receiving from other neural masses, then the effective coupling strength required to initiate seizure activity will be less. Such could be the case in more complex networks.

### 5.4.3 High synaptic gain requires low coupling strength to initiate seizure activity

With the interpretation of the coupling parameter as similar to that of connections between two neuronal populations within one neural mass, it may be thought that the value of this coupling parameter will not likely be greater than  $C_{PY \rightarrow EX}$ , which is the maximum connectivity between populations within a neural mass. For this reason, low- $K$  values could probably be more physiologically plausible. This can in fact be realized by increasing the average synaptic gain  $G_d$  in the post-synaptic impulse response function (Eq. (5.1)). Figure 5.5 shows that the range of  $K$  values for which seizure activity is exhibited is narrower as  $G_d$  is increased and wider as it is decreased from  $G_{PY}$  which is the average synaptic gain of the impulse response function of pyramidal cell population within a neural mass. This suggests that to initiate seizure activity with lower coupling strength values between neural masses, the pyramidal cell population of an afferent neural

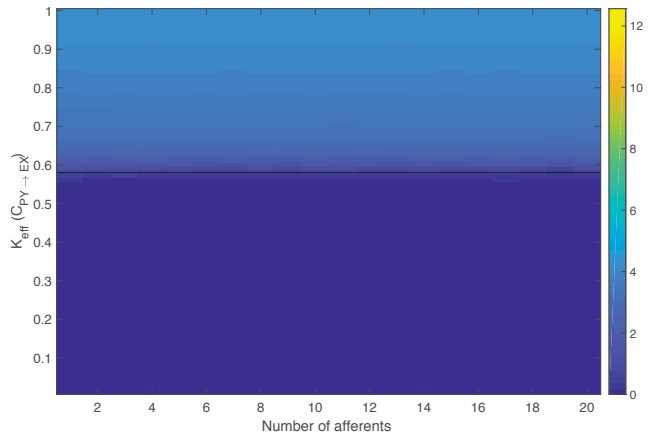
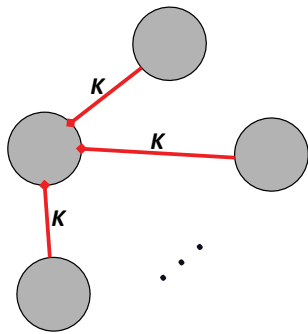
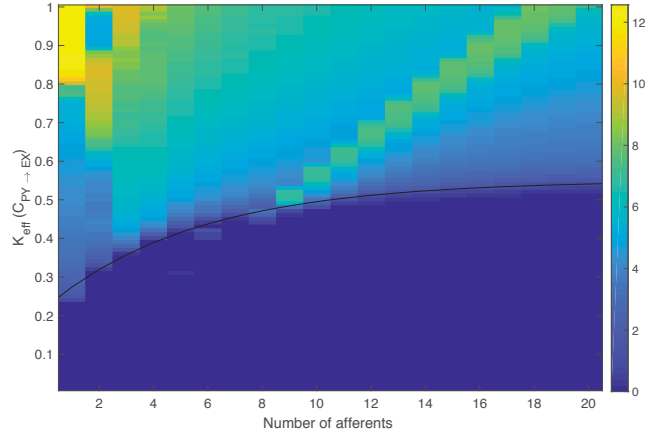
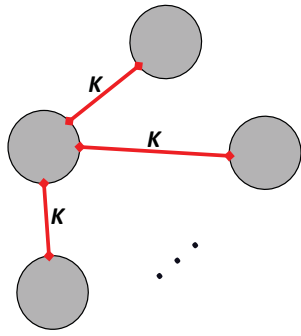


Figure 5.4: Seizure activity initiation from multiple afferents. (Top) Minimum effective coupling strength required to yield seizure activity increases with increasing number of coupled afferent neural masses up to a threshold. (Bottom) Minimum effective coupling strength required to yield seizure activity is the same regardless of the number of afferent neural masses.

mass propagates its activity to the pyramidal cell population of receiving neural mass with greater synaptic gain. This result is mathematically trivial from Eq. (5.7).

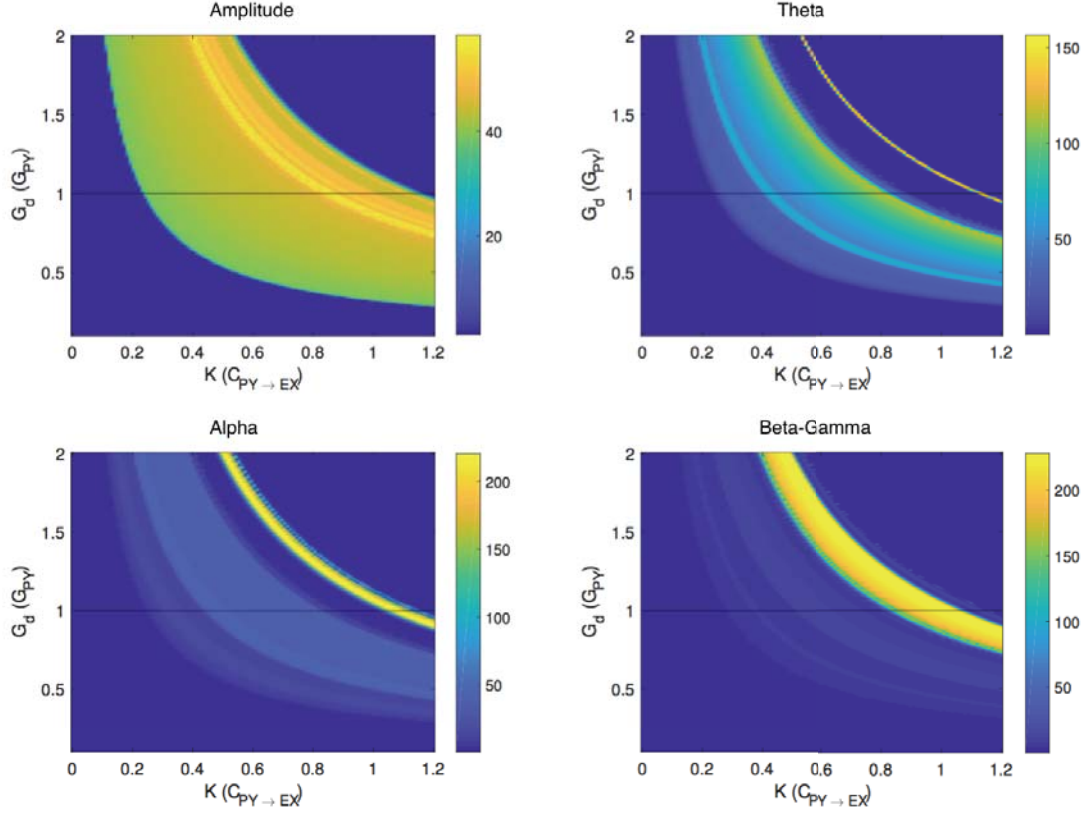


Figure 5.5: Activity map from reciprocally coupled neural masses with varying values of  $G_d$  and  $K$ .

#### 5.4.4 Propagation of seizure activity

We have demonstrated that seizure activity can arise from intrinsic activity of a pathological neural mass or from coupling of two or more neural masses that are not necessarily pathologic. Now, we look at how a neural mass that demonstrates seizure activity propagate this activity to another neural mass that exhibits normal activity when uncoupled. Seizure activity from an afferent source mass is simulated using impaired dendritic inhibition [35] ( $G_{SIN} \in [36, 40]$ ). Note that lower  $G_{SIN}$  yields discharge activity with higher frequency. The strength of uni-directional coupling  $K_{PN}$  from the pathologic mass to the non-pathologic mass

is varied from 0.01 to 0.25. Propagation of seizure activity was quantified by counting the number of discharges, using signal processing methods [93], from the simulated LFP of the coupled neural masses and taking their ratio. In Figure 5.6, we find that a minimum coupling strength around  $0.05C_{PY \rightarrow EX}$  is required to completely propagate the seizure activity to the non-pathologic mass regardless of the degree of pathology of the source mass. It can also be observed that low-frequency discharge activity (around  $G_{SIN} = 40$ ) yields bursting activity when propagated with high coupling strength values.

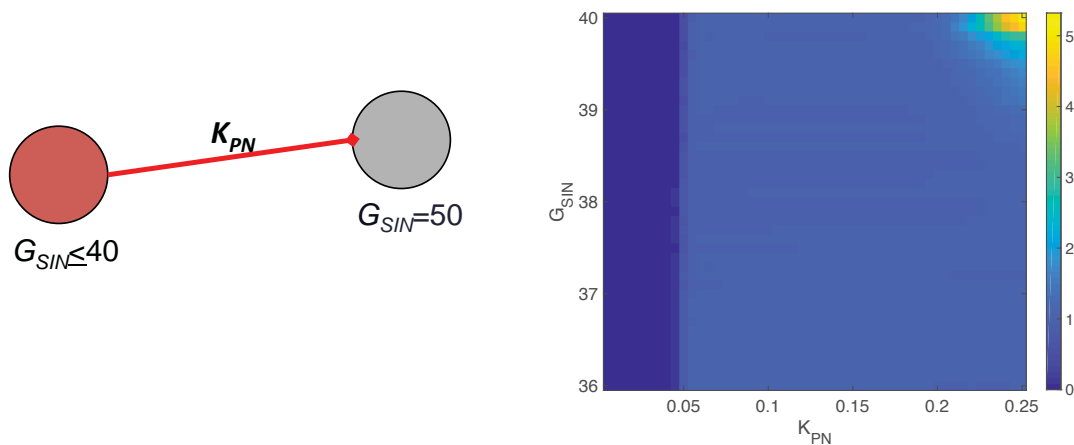


Figure 5.6: Propagation of pathologic discharge activity. A pathologic source mass propagates its discharge activity to a non-pathologic mass with a minimum coupling strength  $K_{PN}$  around  $0.05C_{PY \rightarrow EX}$  regardless of the degree of pathological activity.

There seems to be a substantial difference in the required coupling strength to initiate seizure activity and to propagate it. This difference can play a critical role in the spread of seizure activity in a network of neural masses - it requires a significant strength of coupling to initiate a seizure activity in one brain region but once seizure activity is initiated, it requires lower amount of coupling to propagate it to connected brain regions. To illustrate this, we simulated a grid network of 25 non-pathologic brain regions, each connected to its four nearest neighbors (up, down, top, bottom). The coupling strength from one brain region  $i$  to one of its neighbor  $j$  is randomly set as  $K_{ij} = \frac{1}{4}K_{eff,max}\mathcal{U}[0, 1]$ . Using a fixed

random generator seed, we gradually increase  $K_{eff,max}$  until the network starts to demonstrate seizure activity as shown in Figure 5.7, where  $K_{eff,max} = 0.402$ . Looking at the activities of the neural masses, we can see that discharge activity first appears in the neural mass that has the largest  $K_{eff}$  value (center) and propagates it to its neighbors with high  $K_{eff}$  values (up and right). The propagated seizure activity is then cascaded to connected neural masses satisfying the required minimum effective coupling strength as indicated by the red arrows.

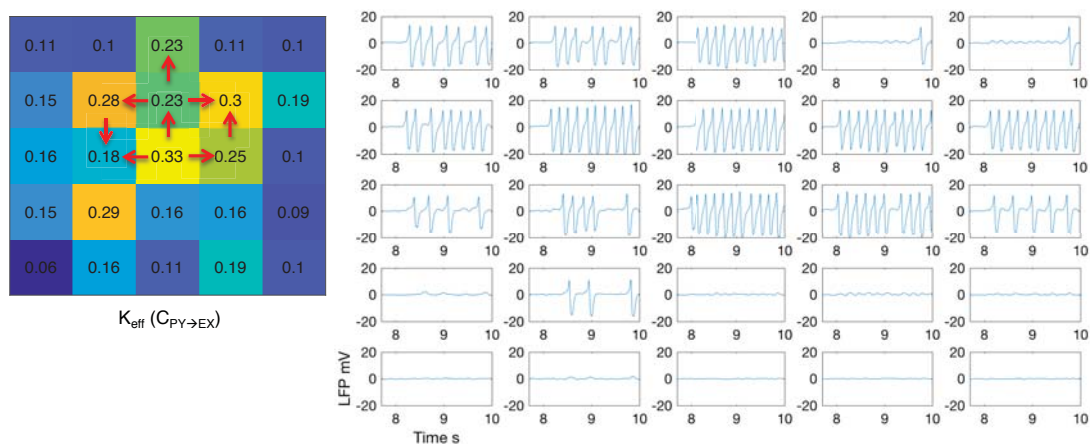


Figure 5.7: Initiation and propagation of discharge activity in a grid network of neural masses. Twenty-five neural masses are arranged in a grid, each connected to their four nearest neighbors with a random coupling strength value. The effective coupling strengths are shown in the left plot.

#### 5.4.5 Effect of focal cooling on the propagation of seizure activity

Using the temperature dependence formulated in Chapter 4, we now investigate whether thermal neuromodulation is effective in the case of spreading seizure activity. By focally cooling a pathologic brain region that demonstrates epileptic discharge activity, we have shown that the temperature dependence in the model simulates suppression of discharge activity as observed in experiments with rats.

Suppression or termination of focally cooled discharge activity depends on the temperature coefficients of the synaptic and intrinsic firing processes of the neural mass model (Chapter 4). We simulate a neural mass that demonstrates epileptic discharge activity and is afferent to a non-pathologic neural mass as in Figure 5.6. Temperature dependent parameters were set to simulate suppression only of discharge activity ( $Q_{10,syn} = Q_{10,int} = 1.8$ ).

In Figure 5.8, we show the amplitude and frequency of the discharge activity of the non-pathologic neural mass. (Discharges whose amplitude is less than 5mV are considered subthreshold and are not included in frequency count.) The figure depicts that focal cooling of the source of seizure activity can stop the propagation of low frequency discharge activity ( $G_{SIN} \in [38.5, 40]$ ). If the discharge activity has higher frequency ( $G_{SIN} \in [36, 38.5]$ ), the minimum coupling strength required to propagate the seizure activity to the connected brain region is increased from  $0.05C_{PY \rightarrow EX}$  to around  $0.15C_{PY \rightarrow EX}$  and  $0.20C_{PY \rightarrow EX}$  with 20°C and 15°C cooling, respectively. Above this coupling strength values, discharges are propagated to the non-pathologic brain region but are lower in both magnitude and frequency. These effects were also observed when we used the original coupling model of Jansen and Rit (not shown). Significance of these simulated effects of focal cooling to ictogenesis is discussed in the following section.

## 5.5 Discussion

The proposed coupling model offers a physiological mechanism that can simulate initiation of seizure activity in a non-pathologic brain region and propagation of seizure activity from one brain region to nearby and distant regions. The model retains the mechanism proposed in Jansen and Rit model that the signal propagated to an connected region is via a different impulse response function. This can translate to axonal sprouting in which axonal processes of a neuron grow out and create synaptic connections with the dendritic processes of other neurons. Interestingly, axonal sprouting phenomenon is observed in temporal lobe epilepsy, both human and animal models [94–96], wherein mossy fibers sprout and form

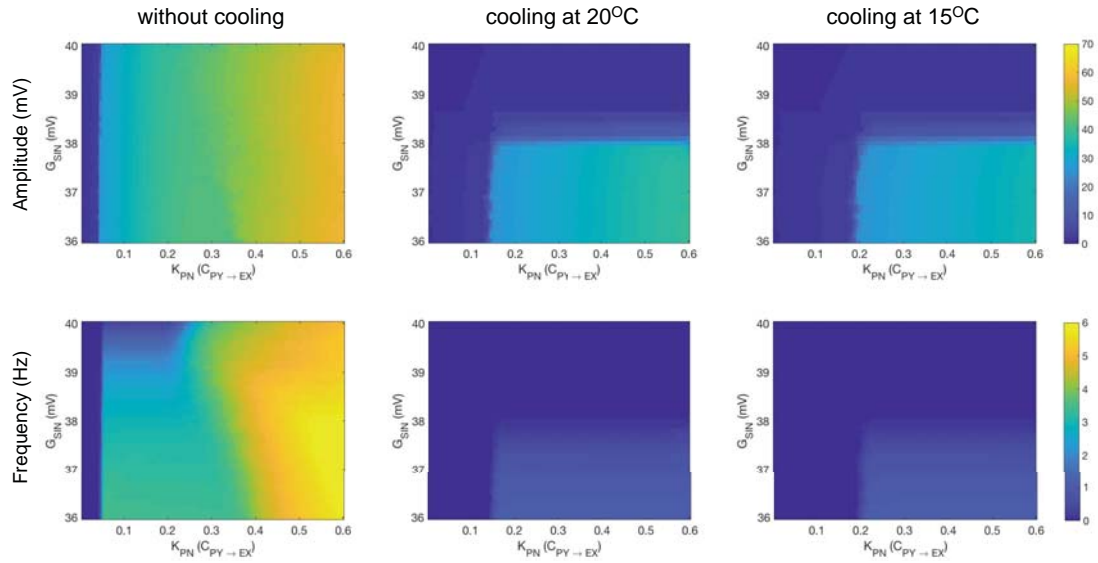


Figure 5.8: Effect of focally cooling the pathologic brain region on the propagation of seizure activity. Focal cooling stops the propagation of low frequency discharge activity while it increases the minimum coupling strength required to propagate high-frequency seizure activity to the connected brain region. Propagated discharges at higher coupling values, on the other hand, are observed with lower amplitude and frequency.

new synapses with denrites in the granule and molecular layers. It is also observed to be induced in CA3 pyramidal cells in a hippocampal lesion [97] and in layer V pyramidal cells of chronically injured epileptogenic rat neocortex [98]. The study by Buckmaster et al. [99] showed that a predominantly excitatory feedback circuit is created via axon sprouting in a TLE model and reported that sprouted mossy fibers project locally and not distally as with normal mossy cell axons. McKinney et al. [97] also reported that lesion-induced axonal sprouting leads to an increased excitatory connection between CA3 pyramidal cells without apparent decrease in synaptic inhibition. These observations somehow validate how our model can generate seizure activity from coupling of two brain regions that are not necessarily pathologic. In contrast to impaired inhibition [35], hyperexcitability still arises via an altered excitation-inhibition balance but in a different way - excita-

tion is increased because of recurrent excitatory connections via axonal sprouting.

We showed that different kinds of seizure activity can actually arise depending only on the strength of reciprocal coupling between two neural masses that initially demonstrate normal activity. Hence, we propose a parsimonious model that can explain how another type of seizure activity such as high-frequency periodic oscillation or waxing and waning oscillations, can evolve from a spontaneous discharge activity for example. Use of ultrastructural studies in hippocampal TLE showed that sprouted axons exhibit formation of aberrant synaptic contacts such as changes in spine morphology, perforated post-synaptic densities, and multiple spine boutons that could be associated with enhancement of synaptic efficiency which is similarly observed in long term potentiation studies [88]. These are possible physiological translations of how hyperexcitability arises from increase in synaptic connectivity or alternatively in synaptic gain as we have shown in Figure 5.5.

We found that the coupling strength required to propagate a seizure activity to a non-pathologic brain region is less than to initiate it. This is a critical finding since it can shed light on how some seizures are localized on one brain hemisphere while some spreads across other brain regions. The effective coupling strength that results from the connectivity of one brain region with other brain regions determines its ability to initiate a seizure activity which it can more easily propagate to brain regions connected from it. It was reported that functional networks constructed from EEG of epilepsy patients revealed significantly higher mean degree compared to control patients [81]. Analogously, effective coupling strength is increased when a brain region has more afferent connections, and it can then potentially initiate seizure activity. In the same way, seizure activity is easier to propagate to a brain region that have more inward connections. This is in agreement to the idea that epilepsy is indeed a network disease and that treatment of intractable epilepsy patients may require individualized connectome-based interventions [100].

We have shown in Chapter 4 that focal cooling can suppress epileptic

discharge activity as consistently shown in animal experiments. However, there have been no experiments that look into the applicability of focal cooling for secondary generalized epilepsy in which seizure activity spreads to other brain regions. The ultimate goal of focal brain cooling studies is to create an implantable device that will cool the epileptogenic foci of the brain when seizure activity is detected. This study investigates whether focal cooling will also be effective for partial epilepsy with secondary generalization. Analysis of the results presented here suggests the affirmative. First, focal cooling was found to stop the propagation of low-frequency discharge activity. This kind of activity is characteristic of interictal spikes. Studies show that interictal spikes foreshadow the occurrence of seizure activity and it is believed that they may drive epileptogenesis since they can induce long-term changes in synaptic connections between neurons [102]. If there is in fact truth to this hypothesis, focal cooling can be utilized as anti-spike therapy not only to prevent or reduce epileptogenesis but also cognitive comorbidity in epilepsy [102]. Second, propagation of focally cooled high-frequency discharge activity to the non-pathological brain region is unhindered but requires more synaptic connections; using 15OC cooling, four times more than the amount of coupling required without cooling. Essentially, this could mean that cooling may be able to stop the propagation of the discharge activity if this amount of coupling results from a spatial recruitment process; i.e. discharges do not get propagated with lower coupling and takes time to achieve the required amount of coupling. Slow spatial recruitment was reportedly observed in a neocortical secondary generalized epilepsy [103]. Proix et al. also suggest that seizure recruitment and propagation is driven at a slow timescale [104]. With stronger coupling, high-frequency subthreshold spikes are amplified and reinforced, and become suprathreshold when propagated. Discharges that are propagated this way, however, were observed to be lower in magnitude and less frequent to occur than without cooling, a result that is still indicative that cooling achieves a therapeutic effect.

# 6 Conclusion

## 6.1 Summary

The ultimate goal of focal brain cooling studies is to realize an implantable cooling device that will be placed at the epileptic region of the brain, implementing a temperature control when a seizure activity is detected. This neuromodulation treatment is seen as a better alternative than surgical resection that involves more cost and high risk. Extensive studies have been made, establishing that cooling can suppress epileptic discharges. This study utilized a computational approach to explain what possible mechanisms with which cooling suppresses or even terminate discharge activity as seen in most *in vitro* studies.

We formulated a temperature dependent neural mass model that reproduces the effect of focal cooling of an animal model of epilepsy *in vivo*. First, based from experimental evidences that cooling reduces neurotransmitter concentrations at the synapses, we used a  $Q_{10}$  factor to attenuate the output of the post-synaptic impulse response function. This attenuation results in reduction of frequency of discharges with no significant suppression of magnitude. Experiments with rats *in vivo*, however, showed that the discharge activity is generally persistent during cooling but the discharge magnitude is clearly suppressed. Some rats even exhibited slight increases in frequency during cooling. This implied that the resulting reduction in frequency of discharges brought by the first mechanism should be compensated, leading us to conjecture a reciprocal  $Q_{10}$  factor multiplied to the input of the firing response function. Such formulation is equivalent to the attenuation of both the average and variability of the firing thresholds of excitation of neurons in the population. Surprisingly, these are supported by earlier studies showing that cooling depolarizes the cell membrane of neurons

bringing them closer to spiking threshold, thus increasing their excitability and decreasing the variability in the excitation levels of neurons across the population.

The model puts forward that the two major processes involved in the neural mass model that simulates epileptic discharge activity may have differential temperature sensitivities, which determine the response of the discharge activity to cooling. Suppression of discharge activity was seen when the intrinsic excitability mechanism just compensates the effect of the synaptic mechanism. Increase in the frequency of discharges results if the intrinsic mechanism overcompensates the effect of the synaptic mechanism while termination of discharge activity results if the intrinsic mechanism undercompensates the effect of the synaptic mechanism.

Seizure activity can start in one brain region and may spread to other brain regions, recruiting a network of propagating nodes. We were interested to investigate whether focal cooling or cooling only the epileptogenic zone, can stop the spread of seizure activity such as in secondary generalized epilepsy. This part of the study required a physiologically interpretable coupling model to simulate propagation of brain activity. We proposed a coupling model that reconciles existing coupling schemes in coupled neural mass models. The proposed method was able to simulate seizure activity initiation in non-pathological brain regions, evolving into other types of seizure activity by further increasing the strength of coupling. The mechanism can encompass axonal sprouting, a firmly established phenomenon associated with seizure activity occurrence in human and animal models of epilepsy and lesion models. We found that a minimum coupling strength is required to initiate a seizure activity in one brain region depending on its connection with afferent brain regions. Moreover, a much lower coupling strength is required to propagate seizure activity to a connected brain regions. The difference between these coupling strength requirements can be crucial in the spread of seizure activity across brain regions. These results may shed some light on how epilepsy can be seen as a network disease, which is the current focus of several recent studies (see Chapter 5).

Finally, we conclude that focal cooling can be an effective treatment for

partial epilepsy including secondary generalized epilepsy cases. It can stop the propagation of low-frequency discharge activity that is suspected to be a driver of epileptogenicity. On the other hand, focal cooling increases the required coupling strength to propagate high-frequency discharge activity which could essentially stop the spread of seizure activity if the spatial recruitment process is slow.

## 6.2 Recommendations

Our computational approach to model the effect of cooling on epileptic discharge activity may be too simplistic. Recent studies on epilepsy and epilepsy models have involved the role of non-neuronal cells such as astrocytes and microglia in the mechanisms of seizure development such as reactive astrogliosis, glial-mediated inflammation, and  $\text{Ca}^{2+}$  signalling dysfunction [106, 107]. It may also be possible that cooling can attenuate activation of both neuronal and non-neuronal cells that will consequently impair their involvement in one or several hyperexcitability mechanisms. While there have been recent attempts at modelling the interaction of neuronal and non-neuronal cells [108, 109], formulation of temperature dependence on the models will require multimodal recordings other than EEG (extracellular GABA and glutamate concentrations, cerebral blood flow) in focal brain cooling experiments to estimate the model parameters.

The second part of the study (Chapter 5), in its current form, is purely *in silico*, which we hope to be validated with experimental and clinical data in the future. Using multi-channel EEG recording from epilepsy patients, we can perform parameter estimation of the model to estimate the coupling strengths between brain regions. We believe that the proposed model could be useful for pre-surgical diagnosis of medically intractable epilepsy patients. This is already possible with the recent technological advances in accurately estimating structural connectivities between brain regions such as advanced diffusion magnetic resonance imaging. We can also come up with an index that could indicate the ictogenicity of one brain region based from its structural connection with other brain regions such as in [83, 85].

The need to verify our findings regarding the feasibility of focal cooling for secondary generalized seizures is imperative if the ultimate goal is to develop an implantable cooling device. Experiments with multi-electrode grid EEG recording during cooling will be necessary to establish this together with an appropriate model for the spatial diffusion of temperature from the cooled brain region to nearby and distant regions.

Capitalizing on the idea that the coupling model used in the study can encompass axonal sprouting, it is interesting to explore the causative relation between seizure activity occurrence and axonal sprouting and investigate the temporal progression of the phenomenon. We could then come up with a time-dependent model of axonal sprouting to simulate a realistic spread of seizure activity. Ultimately, we would like to derive a generative brain network model for secondary generalized epilepsy based on this phenomenon.

### **6.3 Pipeline for proposed thermal neuromodulation**

In Figure 6.1, we propose a pipeline that integrates the results of this study with implantation of focal brain cooling device that will deliver thermal neuromodulation via a temperature control. The pipeline starts with pre-deployment procedures that will delineate the epileptogenic zone (EZ) of a patient's brain. This may require several modalities including scalp EEG and MRI. Once the EZ is delineated, preliminary experiments using focal cooling will be done with intracranial EEG recordings from which the relevant parameters of the model will be estimated offline.

A seizure detection algorithm is independently developed although several seizure detection algorithms have already been proposed to date especially for therapeutic devices (see [105] for review). Any particular method can be rectified or personalized using the recently derived intracranial recordings from the patient.

Additionally, diffusion MRI can be performed to identify potential brain regions that significantly participate in the propagation of seizure activity in patients with secondary generalized epilepsy. Knowledge of this may also help in the optimal placement of one or several cooling devices. Finally, a temperature control will then be developed using the estimated parameters of the model and integrated together with the seizure detection algorithm in the brain cooling device. Thermal neuromodulation will be delivered by the device every time a seizure activity is detected.

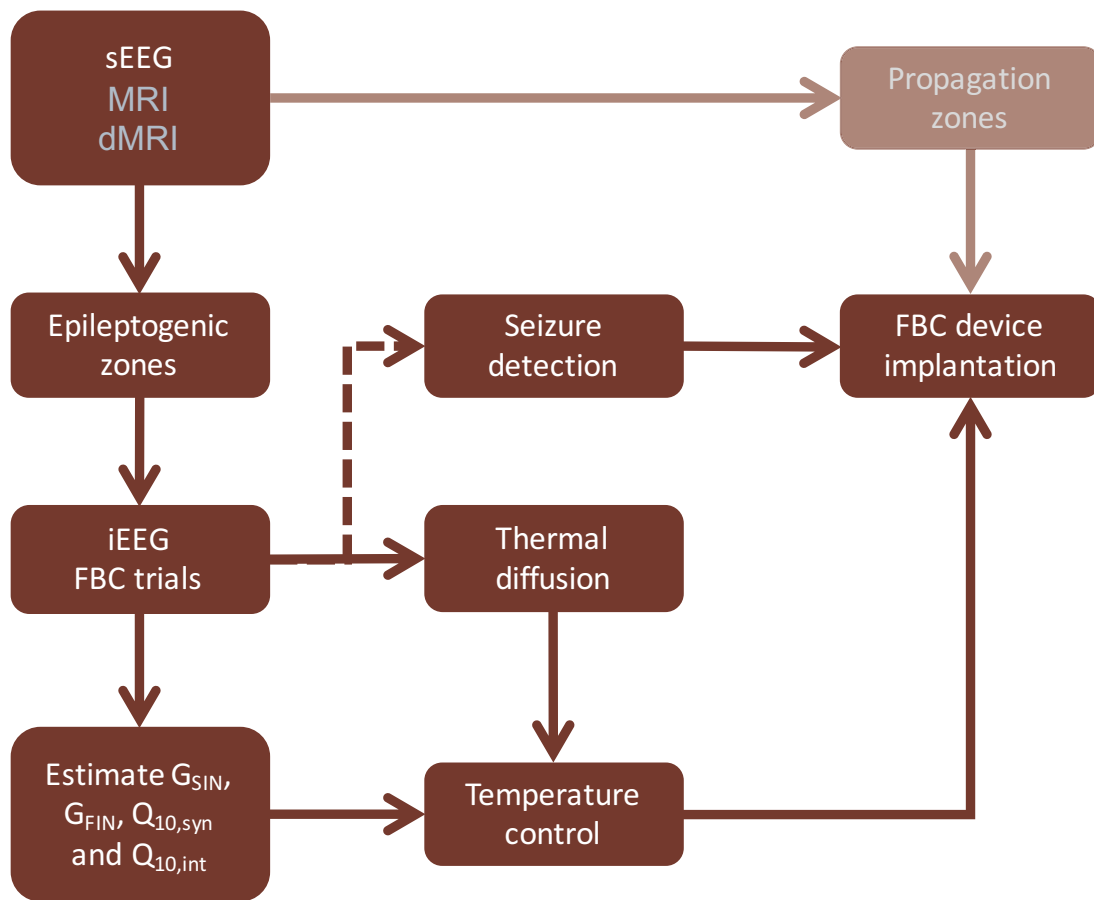


Figure 6.1: Pipeline for proposed thermal neuromodulation for medically intractable epilepsy patients

# Acknowledgements

This study has come to fruition, many thanks to all the people I have worked with and the people who inspired me all throughout the journey. *I am very grateful!*

Ikeda-sensei, thank you for accepting me in the Mathematical Informatics Laboratory and giving me opportunities to hone my knowledge and skills in computational neuroscience.

Sato-sensei, Sakumura-sensei, Yoshimoto-sensei, thank you for all your insightful comments and suggestions during my thesis presentations.

Kubo-sensei, I am very grateful for the training and dedication you have given me in this research. Thank you for the life proverbs you shared and all the assistance you extended during my stay in NAIST. Thank you too and Madoka-san for your friendship.

Sir Adrian, thank you for all your advises even before I embarked on my doctoral studies.

Bryan, Clark, and Jeric, doing research in the lab won't be the same without you guys! Do come back home after graduation and let's do research in the Philippines.

Mathematical Informatics Lab, thank you for the family you provided me during my stay in NAIST. PhD batchmates, four batches of masters students, several waves of interns from different parts of the world. I wish you success in all your endeavors- research and otherwise.

Pinoy@NAIST. It's more fun with fellow Filipinos around.

NAIST International Students Affairs Division especially to Ms. Haruna, Ms. Rika, Ms. Kazumi; Ms. Aya and Ms. Sachiko of Mathematical Informatics Lab; Ms. Dae and Ms. Kath of ERDT; Ms. Grace and Ms. Judith of DCS, thank you for all your assistance especially in making the paper works easier for me.

NAIST, indeed, I have outgrown my limits!

DCS, University of the Philippines-Diliman, ERDT, College of Engineering. Thank you for the scholarship and trust. I'm coming back and I hope to pay forward by working with our students to do state-of-the-art research in the university.

Mervin, Leo, Gina, thank you guys for your friendship.

Corazon Bangayan, Soriano family, and the *familia marunggay*. You constantly inspire me to endeavor more.

Aikeen and Anika, I always give my best for you and because of you.

To the Filipino people, things are looking up.

“And may God supply all your needs according  
to his glorious riches in Christ Jesus!”

Taos-pusong pasasalamat,

JM Soriano

# References

- [1] Epilepsy. WHO Factsheet. February 2016.
- [2] Fisher RS, Acevedo C, Arzimanoglou A, Bogacz A. A practical clinical definition of epilepsy: An International League Against Epilepsy official report. *Epilepsia*. 2014;55:1-8.
- [3] Engel J. Seizures and epilepsy. Oxford University Press; 2013 Jan 31.
- [4] Glauser T, Ben-Menachem E, Bourgeois B, Cnaan A, Guerreiro C, Kalvainen R, Mattson R, French JA, Perucca E, Tomson T. Updated ILAE evidence review of antiepileptic drug efficacy and effectiveness as initial monotherapy for epileptic seizures and syndromes. *Epilepsia*. 2013 Mar 1;54(3):551-63.
- [5] Perucca E, French J, Bialer M. Development of new antiepileptic drugs: challenges, incentives, and recent advances. *The Lancet Neurology*. 2007 Sep 30;6(9):793-804.
- [6] French JA. Refractory epilepsy: clinical overview. *Epilepsia*. 2007 Mar 1;48(s1):3-7.
- [7] Kwan P, Sander JW. The natural history of epilepsy: an epidemiological view. *Journal of Neurology, Neurosurgery & Psychiatry*. 2004 Oct 1;75(10):1376-81.
- [8] Beleza P. Refractory epilepsy: a clinically oriented review. *European neurology*. 2009 Jun 12;62(2):65-71.
- [9] Schuele SU, Luders HO. Intractable epilepsy: management and therapeutic alternatives. *The Lancet Neurology*. 2008 Jun 30;7(6):514-24.

- [10] Spencer S, Huh L. Outcomes of epilepsy surgery in adults and children. *The Lancet Neurology*. 2008 Jun 30;7(6):525-37.
- [11] Noachtar S, Borggraefe I. Epilepsy surgery: a critical review. *Epilepsy & Behavior*. 2009 May 31;15(1):66-72.
- [12] Fridley J, Thomas JG, Navarro JC, Yoshor D. Brain stimulation for the treatment of epilepsy. *Neurosurgical focus*. 2012 Mar;32(3):E13.
- [13] Terry Jr RS. Vagus nerve stimulation therapy for epilepsy. In *Epilepsy Topics* 2014. InTech.
- [14] Motamedi GK, Lesser RP, Vicini S. Therapeutic brain hypothermia, its mechanisms of action, and its prospects as a treatment for epilepsy. *Epilepsia*. 2013 Jun 1;54(6):959-70.
- [15] Wang H, Wang B, Normoyle KP, Jackson K, Spitler K, Sharrock MF, Miller CM, Best C, Llano D, Du R. Brain temperature and its fundamental properties: a review for clinical neuroscientists. *Frontiers in neuroscience*. 2014 Oct 8;8:307.
- [16] Matsui T, Kida H, Iha T, Obara T, Nomura S, Fujimiya T, Suzuki M. Effects of hypothermia on ex vivo microglial production of pro-and anti-inflammatory cytokines and nitric oxide in hypoxic-ischemic brain-injured mice. *Folia neuropathologica/Association of Polish Neuropathologists and Medical Research Centre, Polish Academy of Sciences*. 2014 Jan 1;52(2):151.
- [17] Tanaka N, Fujii M, Imoto H, Uchiyama J, Nakano K, Nomura S, Fujisawa H, Kunitsugu I, Saito T, Suzuki M. Effective suppression of hippocampal seizures in rats by direct hippocampal cooling with a Peltier chip. *Journal of Neurosurgery*. 2008 April 1;108(4):791-797.
- [18] Fujii M, Inoue T, Nomura S, Maruta Y, He Y, Koizumi H, Shirao S, Owada Y, Kunitsugu I, Yamakawa T, Tokiwa T. Cooling of the epileptic focus suppresses seizures with minimal influence on neurologic functions. *Epilepsia*. 2012 Mar 1;53(3):485-93.

- [19] Inoue T, Fujii M, He Y, Maruta Y, Kida H, Nomura S, Suzuki M, Tokiwa T, Yamakawa T, Yamakawa T, Hirano K. Development of a focal cerebral cooling system for the treatment of intractable epilepsy: An experimental study in cats and non-human primates. In Systems, Man, and Cybernetics (SMC), 2011 IEEE International Conference on 2011 Oct 9 (pp. 691-695). IEEE.
- [20] Yang XF, Duffy DW, Morley RE, Rothman SM. Neocortical seizure termination by focal cooling: temperature dependence and automated seizure detection. *Epilepsia*. 2002 Mar 1;43(3):240-5.
- [21] Oku T, Fujii M, Tanaka N, Imoto H, Uchiyama J, Oka F, Kunitsugu I, Fujioka H, Nomura S, Kajiwara K, Fujisawa H. The influence of focal brain cooling on neurophysiopathology: validation for clinical application: Laboratory investigation. *Journal of neurosurgery*. 2009 Jun;110(6):1209-17.
- [22] Fujii M, Fujioka H, Oku T, Tanaka N, Imoto H, Maruta Y, Nomura S, Kajiwara K, Saito T, Yamakawa T, Yamakawa T. Application of focal cerebral cooling for the treatment of intractable epilepsy. *Neurologia medico-chirurgica*. 2010;50(9):839-44.
- [23] D'Ambrosio R, Eastman CL, Darvas F, Fender JS, Verley DR, Farin FM, Wilkerson HW, Temkin NR, Miller JW, Ojemann J, Rothman SM. Mild passive focal cooling prevents epileptic seizures after head injury in rats. *Annals of neurology*. 2013 Feb 1;73(2):199-209.
- [24] Yenari MA, Han HS. Neuroprotective mechanisms of hypothermia in brain ischaemia. *Nature Reviews Neuroscience*. 2012 Apr 1;13(4):267-78.
- [25] Kida H, Nomura S, Shinoyama M, Ideguchi M, Owada Y, Suzuki M. The effect of hypothermia therapy on cortical laminar disruption following ischemic injury in neonatal mice. *PloS one*. 2013 Jul 23;8(7):e68877.
- [26] He Y, Fujii M, Inoue T, Nomura S, Maruta Y, Oka F, Shirao S, Owada Y, Kida H, Kunitsugu I, Yamakawa T. Neuroprotective effects of focal brain cooling on photochemically-induced cerebral infarction in rats: analysis from a neurophysiological perspective. *Brain research*. 2013 Feb 25;1497:53-60.

- [27] Jacobs SE, Hunt R, Tarnow-Mordi WO, Inder TE, Davis PG. Cochrane Review: Cooling for newborns with hypoxic ischaemic encephalopathy. Evidence-Based Child Health: A Cochrane Review Journal. 2008 Dec 1;3(4):1049-115.
- [28] Guttman R. Effect of temperature on the potential and current thresholds of axon membrane. The Journal of general physiology. 1962 Nov 1;46(2):257-66.
- [29] Thompson SM, Masukawa LM, Prince DA. Temperature dependence of intrinsic membrane properties and synaptic potentials in hippocampal CA1 neurons *in vitro*. The Journal of neuroscience. 1985 Mar 1;5(3):817-24.
- [30] Volgushev M, Kudryashov I, Chistiakova M, Mukovski M, Niesmann J, Eysel UT. Probability of transmitter release at neocortical synapses at different temperatures. Journal of neurophysiology. 2004 Jul 1;92(1):212-20.
- [31] Rosen AD. Nonlinear temperature modulation of Na<sup>+</sup> channel kinetics in GH 3 cells. Biochimica et Biophysica Acta (BBA)-Biomembranes. 2001 Apr 2;1511(2):391-6.
- [32] Aihara H, Okada Y, Tamaki N. The effects of cooling and rewarming on the neuronal activity of pyramidal neurons in guinea pig hippocampal slices. Brain research. 2001 Mar 2;893(1):36-45.
- [33] Lopes da Silva FH, Hoeks A, Smits H, Zetterberg LH. Model of brain rhythmic activity. Biological Cybernetics. 1974 Mar 1;15(1):27-37.
- [34] Jansen BH, Rit VG. Electroencephalogram and visual evoked potential generation in a mathematical model of coupled cortical columns. Biological cybernetics. 1995 Sep 1;73(4):357-66.
- [35] Wendling F, Bartolomei F, Bellanger JJ, Chauvel P. Epileptic fast activity can be explained by a model of impaired GABAergic dendritic inhibition. European Journal of Neuroscience. 2002 May 1;15(9):1499-508.
- [36] David O, Friston KJ. A neural mass model for MEG/EEG: coupling and neuronal dynamics. NeuroImage. 2003 Nov 30;20(3):1743-55.

- [37] Moran RJ, Kiebel SJ, Stephan KE, Reilly RB, Daunizeau J, Friston KJ. A neural mass model of spectral responses in electrophysiology. *NeuroImage*. 2007 Sep 1;37(3):706-20.
- [38] Goodfellow M, Schindler K, Baier G. Intermittent spike-wave dynamics in a heterogeneous, spatially extended neural mass model. *Neuroimage*. 2011 Apr 1;55(3):920-32.
- [39] Yang XF, Ouyang Y, Kennedy BR, Rothman SM. Cooling blocks rat hippocampal neurotransmission by a presynaptic mechanism: observations using 2-photon microscopy. *The Journal of physiology*. 2005 Aug 1;567(1):215-24.
- [40] Rothman SM. The therapeutic potential of focal cooling for neocortical epilepsy. *Neurotherapeutics*. 2009 Apr 30;6(2):251-7.
- [41] Nomura S, Fujii M, Inoue T, He Y, Maruta Y, Koizumi H, Suehiro E, Imoto H, Ishihara H, Oka F, Matsumoto M. Changes in glutamate concentration, glucose metabolism, and cerebral blood flow during focal brain cooling of the epileptogenic cortex in humans. *Epilepsia*. 2014 May 1;55(5):770-6.
- [42] Eilers H, Bickler PE. Hypothermia and isoflurane similarly inhibit glutamate release evoked by chemical anoxia in rat cortical brain slices. *The Journal of the American Society of Anesthesiologists*. 1996 Sep 1;85(3):600-7.
- [43] Nomura S, Inoue T, Imoto H, Suehiro E, Maruta Y, Hirayama Y, Suzuki M. Effects of focal brain cooling on extracellular concentrations of neurotransmitters in patients with epilepsy. *Epilepsia*. 2017 Apr 1;58(4):627-34.
- [44] Hill MW, Wong M, Amarakone A, Rothman SM. Rapid Cooling Aborts Seizure-Like Activity in Rodent Hippocampal-Entorhinal Slices. *Epilepsia*. 2000 Oct 1;41(10):1241-8.
- [45] Motamedi GK, Salazar P, Smith EL, Lesser RP, Webber WR, Ortinski PI, Vicini S, Rogawski MA. Termination of epileptiform activity by cooling in rat hippocampal slice epilepsy models. *Epilepsy research*. 2006 Aug 31;70(2):200-10.

- [46] Bligh JO, Johnson KG. Glossary of terms for thermal physiology. *Journal of Applied Physiology*. 1973 Dec 1;35(6):941-61.
- [47] Kida H, Fujii M, Inoue T, He Y, Maruta Y, Nomura S, Taniguchi K, Ichikawa T, Saito T, Yamakawa T, Suzuki M. Focal brain cooling terminates the faster frequency components of epileptic discharges induced by penicillin G in anesthetized rats. *Clinical Neurophysiology*. 2012 Sep 30;123(9):1708-13.
- [48] Wilson HR, Cowan JD. Excitatory and inhibitory interactions in localized populations of model neurons. *Biophysical journal*. 1972 Jan;12(1):1.
- [49] Deco G, Jirsa VK, Robinson PA, Breakspear M, Friston K. The dynamic brain: from spiking neurons to neural masses and cortical fields. *PLoS computational biology*. 2008 Aug 29;4(8):e1000092.
- [50] Miles R, Toth K, Gulyas AI, Hajos N, Freund TF. Differences between somatic and dendritic inhibition in the hippocampus. *Neuron*. 1996 Apr 30;16(4):815-23.
- [51] Banks MI, White JA, Pearce RA. Interactions between distinct GABA A circuits in hippocampus. *Neuron*. 2000 Feb 29;25(2):449-57.
- [52] Markram H, Toledo-Rodriguez M, Wang Y, Gupta A, Silberberg G, Wu C. Interneurons of the neocortical inhibitory system. *Nature Reviews Neuroscience*. 2004 Oct 1;5(10):793-807.
- [53] Wendling F, Hernandez A, Bellanger JJ, Chauvel P, Bartolomei F. Interictal to ictal transition in human temporal lobe epilepsy: insights from a computational model of intracerebral EEG. *Journal of Clinical Neurophysiology*. 2005 Oct;22(5):343.
- [54] Achard P, Van Geit W, LeMasson G. Parameter searching. In: *Computational modeling methods for neuroscientists*, De Schutter E, ed. Cambridge: MIT Press, 2009.
- [55] Jones DR, Perttunen CD, Stuckman BE. Lipschitzian optimization without the Lipschitz constant. *Journal of Optimization Theory and Applications*. 1993 Oct 1;79(1):157-81.

- [56] Finkel, D. DIRECT optimization algorithm user guide. Center for Research in Scientific Computation, North Carolina State University, 2003, 2.
- [57] Lopez-Cuevas A, Castillo-Toledo B, Medina-Ceja L, Ventura-Mejia C. State and parameter estimation of a neural mass model from electrophysiological signals during the status epilepticus. *NeuroImage*. 2015 Jun 30;113:374-86.
- [58] Friston KJ, Harrison L, Penny W. Dynamic causal modelling. *Neuroimage*. 2003 Aug 31;19(4):1273-302.
- [59] Canan S, Ankarali S, Marangoz C. Detailed spectral profile analysis of penicillin-induced epileptiform activity in anesthetized rats. *Epilepsy research*. 2008 Nov 30;82(1):7-14.
- [60] Cossart R, Dinocourt C, Hirsch JC, Merchan-Perez A, De Felipe J, Ben-Ari Y, Esclapez M, Bernard C. Dendritic but not somatic GABAergic inhibition is decreased in experimental epilepsy. *Nature neuroscience*. 2001 Jan 1;4(1):52-62.
- [61] Dhooge A, Govaerts W, Kuznetsov YA. MATCONT: a MATLAB package for numerical bifurcation analysis of ODEs. *ACM Transactions on Mathematical Software (TOMS)*. 2003 Jun 1;29(2):141-64.
- [62] Bak LK, Schousboe A, Waagepetersen HS. The glutamate/GABA-glutamine cycle: aspects of transport, neurotransmitter homeostasis and ammonia transfer. *Journal of neurochemistry*. 2006 Aug 1;98(3):641-53.
- [63] Weight FF, Erulkar SD. Synaptic transmission and effects of temperature at the squid giant synapse. *Nature*. 1976 Jun 24;261(5562):720-2.
- [64] Rinberg A, Taylor A, & Marder E. The effects of temperature on the stability of a neuronal oscillator. *PLoS computational biology*. 2013; 9(1), e1002857.
- [65] Braun HA, Huber MT, Dewald M, Schafer K, Voigt K. Computer simulations of neuronal signal transduction: the role of nonlinear dynamics and noise. *International Journal of Bifurcation and Chaos*. 1998 May;8(05):881-9.

- [66] Sato YD, Okumura K, Ichiki A, Shiino M, Cateau H. Temperature-modulated synchronization transition in coupled neuronal oscillators. *Physical Review E*. 2012 Mar 15;85(3):031910.
- [67] Barbour B, Hausser M. Intersynaptic diffusion of neurotransmitter. *Trends in neurosciences*. 1997 Sep 1;20(9):377-84.
- [68] Triller A, Choquet D. New concepts in synaptic biology derived from single-molecule imaging. *Neuron*. 2008 Aug 14;59(3):359-74.
- [69] Murphy-Royal C, Dupuis JP, Varela JA, Panatier A, Pinson B, Baufreton J, Groc L, Oliet SH. Surface diffusion of astrocytic glutamate transporters shapes synaptic transmission. *Nature neuroscience*. 2015 Feb 1;18(2):219-26.
- [70] Shen KF, Schwartzkroin PA. Effects of temperature alterations on population and cellular activities in hippocampal slices from mature and immature rabbit. *Brain research*. 1988 Dec 20;475(2):305-16.
- [71] Volgushev M, Vidyasagar TR, Chistiakova M, Yousef T, Eysel UT. Membrane properties and spike generation in rat visual cortical cells during reversible cooling. *The Journal of Physiology*. 2000 Jan 1;522(1):59-76.
- [72] Henze DA, Buzsaki G. Action potential threshold of hippocampal pyramidal cells in vivo is increased by recent spiking activity. *Neuroscience*. 2001 Jul 16;105(1):121-30.
- [73] Yu Y, Shu Y, McCormick DA. Cortical action potential backpropagation explains spike threshold variability and rapid-onset kinetics. *Journal of Neuroscience*. 2008 Jul 16;28(29):7260-72.
- [74] Sarria I, Ling J, Gu JG. Thermal sensitivity of voltage-gated Na<sup>+</sup> channels and A-type K<sup>+</sup> channels contributes to somatosensory neuron excitability at cooling temperatures. *Journal of neurochemistry*. 2012 Sep 1;122(6):1145-54.
- [75] Waters J, Schaefer A, Sakmann B. Backpropagating action potentials in neurones: measurement, mechanisms and potential functions. *Progress in biophysics and molecular biology*. 2005 Jan 31;87(1):145-70.

- [76] Kole MH, Ilshner SU, Kampa BM, Williams SR, Ruben PC, Stuart GJ. Action potential generation requires a high sodium channel density in the axon initial segment. *Nature neuroscience*. 2008 Feb 1;11(2):178-86.
- [77] Collins CA, Rojas E. Temperature dependence of the sodium channel gating kinetics in the node of Ranvier. *Experimental Physiology*. 1982 Jan 22;67(1):41-55.
- [78] Motamedi GK, Gonzalez-Sulser A, Dzakpasu R, Vicini S. Cellular mechanisms of desynchronizing effects of hypothermia in an in vitro epilepsy model. *Neurotherapeutics*. 2012 Jan 1;9(1):199-209.
- [79] Benjamin O, Fitzgerald TH, Ashwin P, Tsaneva-Atanasova K, Chowdhury F, Richardson MP, Terry JR. A phenomenological model of seizure initiation suggests network structure may explain seizure frequency in idiopathic generalised epilepsy. *The Journal of Mathematical Neuroscience*. 2012 Dec 1;2(1):1.
- [80] Terry JR, Benjamin O, Richardson MP. Seizure generation: the role of nodes and networks. *Epilepsia*. 2012 Sep 1;53(9).
- [81] Petkov G, Goodfellow M, Richardson MP, Terry JR. A critical role for network structure in seizure onset: a computational modeling approach. *Frontiers in neurology*. 2014;5.
- [82] Hebbink J, Meijer H, Huiskamp G, Gils S, Leijten F. Phenomenological network models: Lessons for epilepsy surgery. *Epilepsia*. 2017 Oct 1;58(10).
- [83] Goodfellow M, Rummel C, Abela E, Richardson MP, Schindler K, Terry JR. Estimation of brain network ictogenicity predicts outcome from epilepsy surgery. *Scientific reports*. 2016 Jul 7;6:29215.
- [84] Wendling F, Bellanger JJ, Bartolomei F, Chauvel P. Relevance of nonlinear lumped-parameter models in the analysis of depth-EEG epileptic signals. *Biological cybernetics*. 2000 Sep 1;83(4):367-78.

- [85] Lopes MA, Richardson MP, Abela E, Rummel C, Schindler K, Goodfellow M, Terry JR. An optimal strategy for epilepsy surgery: Disruption of the rich-club? *PLoS computational biology*. 2017 Aug 17;13(8):e1005637.
- [86] Goodfellow M, Schindler K, Baier G. Self-organised transients in a neural mass model of epileptogenic tissue dynamics. *NeuroImage*. 2012 Feb 1;59(3):2644-60.
- [87] Sutula T. Seizure-Induced Axonal Sprouting: Assessing Connections Between Injury, Local Circuits, and Epileptogenesis. *Epilepsy currents*. 2002 May 1;2(3):86-91.
- [88] Leite JP, Neder L, Arisi GM, Carlotti CG, Assirati JA, Moreira JE. Plasticity, synaptic strength, and epilepsy: what can we learn from ultrastructural data? *Epilepsia*. 2005 Jul 1;46(s5):134-41.
- [89] Bettus G, Wendling F, Guye M, Valton L, Regis J, Chauvel P, Bartolomei F. Enhanced EEG functional connectivity in mesial temporal lobe epilepsy. *Epilepsy research*. 2008 Sep 30;81(1):58-68.
- [90] Janz P, Schwaderlapp N, Heining K, Haussler U, Korvink JG, von Elverfeldt D, Hennig J, Egert U, LeVan P, Haas CA. Early tissue damage and microstructural reorganization predict disease severity in experimental epilepsy. *eLife*. 2017;6.
- [91] Hutchinson EB, Schwerin SC, Avram AV, Juliano SL, Pierpaoli C. Diffusion MRI and the detection of alterations following traumatic brain injury. *Journal of Neuroscience Research*. 2017 Jun 13.
- [92] Cao Y, Ren K, Su F, Deng B, Wei X, Wang J. Suppression of seizures based on the multi-coupled neural mass model. *Chaos: An Interdisciplinary Journal of Nonlinear Science*. 2015 Oct;25(10):103120.
- [93] O’Haver T. *A Pragmatic introduction to signal processing*. (1997).
- [94] Sutula T, He XX, Cavazos J, Scott G. Synaptic reorganization in the hippocampus induced by abnormal functional activity. *Science*. 1988 Mar 4;239(4844):1147-50.

- [95] Houser CR, Miyashiro JE, Swartz BE, Walsh GO, Rich JR, Delgado-Escueta AV. Altered patterns of dynorphin immunoreactivity suggest mossy fiber reorganization in human hippocampal epilepsy. *Journal of Neuroscience*. 1990 Jan 1;10(1):267-82.
- [96] Cavazos JE, Golarai G, Sutula TP. Mossy fiber synaptic reorganization induced by kindling: time course of development, progression, and permanence. *Journal of Neuroscience*. 1991 Sep 1;11(9):2795-803.
- [97] McKinney RA, Debanne D, Gahwiler BH, Thompson SM. Lesion-induced axonal sprouting and hyperexcitability in the hippocampus in vitro: implications for the genesis of posttraumatic epilepsy. *Nature medicine*. 1997 Sep 1;3(9):990-6.
- [98] Jin X, Prince DA, Huguenard JR. Enhanced excitatory synaptic connectivity in layer V pyramidal neurons of chronically injured epileptogenic neocortex in rats. *Journal of Neuroscience*. 2006 May 3;26(18):4891-900.
- [99] Buckmaster PS, Zhang GF, Yamawaki R. Axon sprouting in a model of temporal lobe epilepsy creates a predominantly excitatory feedback circuit. *Journal of Neuroscience*. 2002 Aug 1;22(15):6650-8.
- [100] Proix T, Bartolomei F, Guye M, & Jirsa V. K. Individual brain structure and modelling predict seizure propagation. *Brain*. 2017. 140(3), 641-654.
- [101] Keranen, T., Sillanpaa, M., & Riekkinen, P. J. Distribution of seizure types in an epileptic population. *Epilepsia*. 1988. 29(1), 1-7.
- [102] Staley K, Hellier JL, Dudek FE. Do interictal spikes drive epileptogenesis? *The Neuroscientist*. 2005 Aug;11(4):272-6.
- [103] Martinet L, et al. Slow spatial recruitment of neocortex during secondarily generalized seizures and its relation to surgical outcome. *Journal of Neuroscience*. 2015; 35(25):9477-9490.
- [104] Proix T, Bartolomei F, Chauvel P, Bernard C, Jirsa VK. Permittivity coupling across brain regions determines seizure recruitment in partial epilepsy. *Journal of Neuroscience*. 2014 Nov 5;34(45):15009-21.

- [105] Gadhoumi, K., Lina, J. M., Mormann, F., & Gotman, J. (2016). Seizure prediction for therapeutic devices: A review. *Journal of neuroscience methods*, 260, 270-282.
- [106] Devinsky O, Vezzani A, Najjar S, De Lanerolle NC, Rogawski MA. Glia and epilepsy: excitability and inflammation. *Trends in neurosciences*. 2013 Mar 31;36(3):174-84.
- [107] Bazargani N, Attwell D. Astrocyte calcium signaling: the third wave. *Nature neuroscience*. 2016 Feb 1;19(2):182-9.
- [108] Blanchard S, SAILLET S, Ivanov A, Benquet P, Benar CG, Pelegrini-Issac M, Benali H, Wendling F. A new computational model for neuro-glio-vascular coupling: astrocyte activation can explain cerebral blood flow nonlinear response to interictal events. *PloS one*. 2016 Feb 5;11(2):e0147292.
- [109] Garnier A, Vidal A, Benali H. A theoretical study on the role of astrocytic activity in neuronal hyperexcitability by a novel neuron-glia mass model. *The Journal of Mathematical Neuroscience*. 2016 Dec 1;6(1):10.

## Publication List

[1] Soriano J, Kubo T, Inoue T, Kida H, Yamakawa T, Suzuki M, Ikeda K. (2017) Differential temperature sensitivity of synaptic and firing processes in a neural mass model of epileptic discharges explains heterogeneous response of experimental epilepsy to focal brain cooling. *PLoS Computational Biology* 13(10): e1005736. <https://doi.org/10.1371/journal.pcbi.1005736>

## Conference List

[1] Soriano J, Kubo T, Inoue T, Kida H, Yamakawa T, Suzuki M, Ikeda K: Bifurcations in a temperature-dependent neural mass model reveal heterogeneous effect of focal cooling on epileptic discharges. *BMC Neuroscience* 2017, 18(Suppl 1): P114.

[2] Soriano J, Kubo T, Inoue T, Kida H, Yamakawa T, Suzuki M, Ikeda K: A temperature-dependent neural mass model for suppression of epileptic discharges. Program No. 407.03. 2016 Neuroscience Meeting Planner. San Diego, CA: Society for Neuroscience, 2016. Online.